Gilbert damping in magnetic layered systems

E. Barati,[1,*] M. Cinal,[1] D. M. Edwards,[2] and A. Umerski[3]
[1]*Institute of Physical Chemistry of the Polish Academy of Sciences, 01-224 Warsaw, Poland*
[2]*Department of Mathematics, Imperial College, London SW7 2BZ, United Kingdom*
[3]*Department of Mathematics and Statistics, Open University, Milton Keynes MK7 6AA, United Kingdom*
(Received 12 April 2014; published 16 July 2014)

The Gilbert damping constant present in the phenomenological Landau-Lifshitz-Gilbert equation describing the dynamics of magnetization is calculated for ferromagnetic metallic films as well as Co/nonmagnet (NM) bilayers. The calculations are done within a realistic nine-orbital tight-binding model including spin-orbit coupling. The convergence of the damping constant expressed as a sum over the Brillouin zone is remarkably improved by introducing finite temperature into the electronic occupation factors and subsequent summation over the Matsubara frequencies. We investigate how the Gilbert damping constant depends on the ferromagnetic film thickness as well as on the thickness of the nonmagnetic cap in Co/NM bilayers (NM = Cu, Pd, Ag, Pt, and Au). The obtained theoretical dependence of the damping constant on the electron-scattering rate, describing the average lifetime of electronic states, varies substantially with the ferromagnetic film thickness and it differs significantly from the dependence for bulk ferromagnetic metals. The presence of nonmagnetic caps is found to largely enhance the magnetic damping in Co/NM bilayers in accordance with experimental data. Unlike Cu, Ag, and Au a particularly strong enhancement is obtained for Pd and Pt caps. This is attributed to the combined effect of the large spin-orbit couplings of Pd and Pt and the simultaneous presence of *d* states at the Fermi level in these two metals. The calculated Gilbert damping constant also shows an oscillatory dependence on the thicknesses of both ferromagnetic and nonmagnetic parts of the investigated systems which is attributed to quantum-well states. Finally, the expression for contributions to the damping constant from individual atomic layers is derived. The obtained distribution of layer contributions in Co/Pt and Co/Pd bilayers proves that the enhanced damping which affects the dynamics of the magnetization in the Co film originates mainly from a region within the nonmagnetic part of the bilayer. Such a nonlocal damping mechanism, related to spin pumping, is almost absent in other investigated bilayers: Co/Cu, Co/Ag, and Co/Au.

DOI: 10.1103/PhysRevB.90.014420 PACS number(s): 75.70.−i, 75.78.−n, 75.40.Gb, 75.70.Tj

I. INTRODUCTION

The dynamics of magnetization in magnetic metallic nanostructures is driven by external stimuli, such as magnetic fields or electric currents as well as by intrinsic relaxation mechanisms. The effective magnetic field, due to external sources and stray fields related to the system's geometry, leads to the Larmor precession of the magnetization vector. The effect of an electric current on magnetization is more subtle since it emerges due to different density and mobility of charge carriers with different spins, i.e., electrons at the Fermi level in ferromagnetic metals included in nanostructures. As a result, net spin currents are present and they transfer spin angular momentum between different parts of the system. The resultant spin-transfer torques can strongly influence the dynamics of magnetization and even lead to its reversal if the current density is sufficiently large. The current-induced reversal of magnetization has been observed, e.g., in nanopillars composed of Co/Ni and Co/Pt multilayers [1].

The processes of magnetization relaxation and switching are profoundly affected by magnetic damping. The time evolution of magnetization $\boldsymbol{M}$ in ferromagnetic metallic systems is well described by the phenomenological Landau-Lifshitz-Gilbert (LLG) equation which includes the damping term $\alpha \boldsymbol{M} \times d\boldsymbol{M}/dt$ introduced by Gilbert [2,3]. This term represents a torque which drives the magnetization vector towards the direction of the effective magnetic field $\boldsymbol{H}_{\mathrm{eff}}$ and its strength is given by the damping constant α. The Gilbert damping plays a key role in the spin dynamics of magnetic systems. In particular, it affects the domain-wall velocity in current-carrying domain-wall structures where fast propagation of domain walls is of great importance for applications in high-speed spintronic devices such as magnetic racetrack memory [4].

It is commonly assumed that the origin of the Gilbert damping is the spin-orbit (SO) coupling. This relativistic effect leads to spin-flip scattering of electrons which results in transfer of angular momentum and energy from spin degrees of freedom to the lattice. The damping constant α is expressed in terms of the spin-orbital torque operator within the quantum-mechanical theory developed by Kamberský and called the torque-correlation model [5,6]. A different way to describe the effect of the SO coupling on damping is a direct calculation of the spin-relaxation torque [7] or determination of spin-wave spectrum from the transverse magnetic susceptibility obtained numerically within the random-phase approximation [8,9]. Another source of magnetic damping in metallic systems is two-magnon scattering [10–12]. It refers to scattering of a uniform magnetization precession mode into pairs of magnons with nonzero wave vectors but it is effective only if the system's translational symmetry is disturbed by structural defects, like film surface roughness.

The Gilbert damping constant α can be determined experimentally from the ferromagnetic resonance (FMR) linewidth

*Corresponding author: ebaratie@gmail.com

(specifically from its term linear in frequency) or by using time-resolved magneto-optical Kerr effect (TRMOKE). Magnetic damping is found to be enhanced, in comparison to bulk ferromagnetic metals, in numerous ferromagnet/nonmagnet (FM/NM) bilayers or multilayers [13–28]. In particular, this concerns Co/Ni, Co/Pd, and Co/Pt layered systems [17,22,23], which also exhibit large perpendicular magnetic anisotropy (PMA) [29–31] as well as large magneto-optical Kerr effect (MOKE) [32]. These observations strongly support the existence of the link between the Gilbert damping and the SO interaction since the latter is responsible for the occurrence of PMA and large MOKE. A clear experimental evidence of such a link is given in Ref. [18] where the quadratic dependence of the damping constant on the SO coupling strength is found for $L1_0$ $FePd_xPt_{1-x}$ ordered alloy films in TRMOKE measurements. Enhanced magnetic damping has also been observed with FMR for tetragonal Ni films on the Cu(001) substrate [14] and bcc Fe films on Ag(001) [15,16] as well as Cu/Py/Cu and Cu/Py/Cu/Pt layered structures [21]. Experimental reports on the Gilbert damping in other systems, including Co/Cu and Py/Cu bilayers, can be found in Refs. [13,19,20,24–28].

The enhancement of Gilbert damping in FM/NM layered structures is attributed to nonlocal damping occurring in the nonmagnet which was predicted theoretically by Berger [33]. The mechanism of damping enhancement proposed by him is based on an idealized picture where conduction *sp* electrons are coupled by exchange to localized *d* electrons forming magnetic moments in the ferromagnet and carry spin through the FM/NM interface to the nonmagnet where it is dissipated. A similar approach based on *s*-*d* exchange coupling and linear-response theory is presented in Refs. [34] and [35] where expressions for the Gilbert damping constant of an NM/FM/NM multilayer are obtained within free-electron models. In Refs. [36], a model based on the idea of spin pumping, from the ferromagnet into adjacent nonmagnetic normal-metal layer, is introduced to explain the enhanced Gilbert damping in NM/FM and NM/FM/NM systems. Based on this theory, the spin emitted into the nonmagnet due to the precession of magnetization in the ferromagnet may either scatter back to the ferromagnet or relax in the adjacent nonmagnet which then acts as a spin sink. The effective magnetic damping is then considered as the sum of intrinsic damping (corresponding to bulk ferromagnet) and the additional damping term which is due to spin pumping and decays as the inverse of the ferromagnetic film thickness [27,36]. A known major factor in this damping process is the spin-diffusion length λ_{sd} of the nonmagnet [13] since to achieve effective relaxation of magnetization due to spin pumping the thickness of the nonmagnetic layer needs to be greater than λ_{sd}. The spin-pumping theory is now commonly used in interpretation and analysis of magnetic damping experimental results [13,22,23,28,37]. It has also been applied in first-principles calculations of the Gilbert damping in Fe/Au, Co/Cu bilayers and trilayers [38]. Although the spin pumping theory provides a simple explanation of nonlocal magnetic damping in nonmagnetic metals in contact with ferromagnetic metals, it does not include a quantum description of the SO coupling responsible for spin relaxation. Instead, the relaxation mechanism is represented only with a phenomenological spin-flip relaxation time. Thus, fully quantum calculations including the SO coupling, like the torque-correlation model, should give an insight into the damping processes on a more fundamental level.

The torque-correlation model or its variations (with α treated as a tensor quantity) has been applied in several theoretical studies for bulk ferromagnets [39–45], half metals [46], transition metal binary alloys [45], $Fe_{1-x}Si_x$ films [47], as well as, very recently, surfaces of ferromagnetic metals [44]. However, this quantum-mechanical approach has hardly been used to study the Gilbert damping and its enhancement in transition metal layered systems. The sole exception is a recent short report [43] by the present authors where the calculated Gilbert damping constant α is shown to be enhanced, with respect to bulk fcc Co, in (001) fcc Co films, both free-standing and covered with a Pd overlayer two monolayers (ML) thick. A similar system of a Co film on the Pd(001) substrate is studied theoretically in Ref. [9] where the spin-wave frequency and its linewidth, proportional to α, are found from the transverse magnetic susceptibility.

In a previous work by one of the authors [48], expressions for various coefficients in the extended LLG equation were obtained by considering the solution for a long-wavelength spin wave in a one-band model. In the present paper, an explicit expression for the Gilbert damping constant in magnetic multilayer systems is found within a realistic nine-band tight-binding (TB) model. The results are reported for purely ferromagnetic metallic films of Fe, Co, and Ni as well as for Co/NM bilayers with the caps of NM = Cu, Pd, Ag, Pt, and Au. They are compared with damping constants found for bulk ferromagnetic metals which were shown in our previous work [43] to agree well with the results of the *ab initio* calculations [39]. The dependence of the Gilbert damping constant on film thickness and the effect of nonmagnetic caps, including the role of their SO coupling, are studied and compared to recent experiments. We also investigate the real-space distribution of the Gilbert damping in layered systems. For this purpose, an explicit expression for contributions to the damping constant from individual atomic layers is derived within the TB model and they are calculated for the investigated films and bilayers. A relation of the obtained results to the predictions of the spin pumping theory is also briefly discussed.

II. THEORY

A. Macroscopic description of magnetization dynamics

Magnetization dynamics of metallic systems can be described with the phenomenological Landau-Lifshitz-Gilbert (LLG) equation. Here, we employ an extended form of this equation,

$$\frac{\partial \boldsymbol{m}}{\partial t} = -\gamma\, \boldsymbol{m} \times \boldsymbol{H}_{\text{eff}} + \alpha\, \boldsymbol{m} \times \frac{\partial \boldsymbol{m}}{\partial t} + 2A\, \boldsymbol{m} \times \frac{\partial^2 \boldsymbol{m}}{\partial x^2} - v_0 \frac{\partial \boldsymbol{m}}{\partial x} + \beta v_0\, \boldsymbol{m} \times \frac{\partial \boldsymbol{m}}{\partial x}, \tag{1}$$

where $\boldsymbol{m} = \boldsymbol{M}/M_s$ denotes the unit vector along the direction of magnetization $\boldsymbol{M}$ (with M_s as its saturation value), γ is the gyromagnetic ratio, and A is the exchange stiffness constant. Other terms can also be included in a further extension of the LLG equation [48]. In the case of a layered system the

magnetization direction $\boldsymbol{m}$ is assumed to vary in the x direction, parallel to the film surface.

Different terms in Eq. (1) account for different torques exerted on the magnetization. The first term describes the Larmor precession of magnetization around the effective magnetic field $\boldsymbol{H}_{\rm eff}$, applied externally and/or due to the intrinsic magnetic anisotropy. The relaxation of magnetization is described by the second term, known as the Gilbert damping which is characterized by the damping constant α. The remaining terms in Eq. (1) are effective only for inhomogeneous magnetization $\boldsymbol{m}(x)$ as in spin waves or domain walls. The fourth and the fifth terms, proposed by Zhang and Li [49], describe adiabatic and nonadiabatic spin-transfer torques, respectively. They both arise due to the flow of the electric current J, with finite spin polarization P, in ferromagnets, and depend on J and P through the parameter $v_0 = g\mu_{\rm B}PJ/(2eM_{\rm s})$ where g is the Landé factor, e is the electric charge, and μ_B is the Bohr magneton. Although the domain-wall velocity is independent of the adiabatic term, it can be controlled by the nonadiabatic term. It is known [50] that the domain-wall velocity is proportional to the parameter β and inversely proportional to the damping constant α [$v = (\beta/\alpha)v_0$]. Thus, both α and β are crucial for a proper description of the magnetization dynamics. Microscopically, the two constants α and β describing the efficiency of magnetic damping and nonadiabatic spin-transfer torque, respectively, arise due to the same interaction, i.e., the SO coupling.

The Gilbert damping constant α is of the main interest in this paper. The effective field $\boldsymbol{H}_{\rm eff}$ and, consequently, the equilibrium direction of magnetization $\boldsymbol{M}$ are assumed to be along the z axis perpendicular to the film surface. Calculations for arbitrary direction of $\boldsymbol{M}$ are presented elsewhere [51].

B. Tight-binding model of electronic structure in magnetic layered systems

In the TB model, the one-electron Hamiltonian H describing an N-monolayer system is represented by its matrix elements in the basis of orthonormalized atomic orbitals $|lj\mu\sigma\rangle$. The basis orbitals of s, p, and d symmetry are localized at the position $\boldsymbol{R}_{lj}$ of each atom j in every layer l. They are labeled with the orbital index $\mu = s,x,y,z,xy,yz,zx,x^2-y^2,3z^2-r^2$ and the spin index $\sigma = \uparrow,\downarrow$.

The matrix elements of the Hamiltonian between orbitals on first- and second-nearest neighbors are found within the Slater-Koster approach [52] using the two-center hopping integrals obtained by fitting *ab initio* energy bands of bulk metals [53]. In the case where neighboring atoms in a layered system are of different metals, each two-center integral $T_{\eta\sigma}$ [$\eta = ss\sigma, pp(\sigma,\pi), dd(\sigma,\pi,\delta), sp(\sigma,\pi), sd(\sigma,\pi,\delta), pd(\sigma,\pi,\delta)$; here σ denotes orbital symmetry not spin] is given by the geometric mean $T_{\eta\sigma} = \pm\sqrt{T^{(1)}_{\eta\sigma}T^{(2)}_{\eta\sigma}}$ when the corresponding integrals $T^{(1)}_{\eta\sigma}, T^{(2)}_{\eta\sigma}$ for the two metals are of the same sign [54,55]. If their signs are opposite the arithmetic mean $T_{\eta\sigma} = \frac{1}{2}(T^{(1)}_{\eta\sigma} + T^{(2)}_{\eta\sigma})$ is taken instead. The two-center hopping integrals $T_{\eta\sigma}$ and the on-site energies $\epsilon_{\mu\sigma}$ obtained by the fit for ferromagnetic metals depend on spin σ. However, since no fit is given in Ref. [53] for ferromagnetic fcc Co, a modified version of the spin-independent parameters T_η, ϵ_μ for paramagnetic fcc Co is used. This is done by taking $T_{\eta\sigma} = T_\eta$, $\epsilon_{\mu\uparrow} = \epsilon_\mu - \frac{1}{2}\Delta_{ex}$, and $\epsilon_{\mu\downarrow} = \epsilon_\mu + \frac{1}{2}\Delta_{ex}$ for d orbitals where $\Delta_{ex} = 1.8$ eV is the exchange splitting for fcc Co [56–58] while assuming $T_{\eta\sigma} = T_\eta$ and $\epsilon_{\mu\sigma} = \epsilon_\mu$ for s and p orbitals.

Due to the two-dimensional (2D) translational symmetry (i.e., in plane in the case of layered systems) the eigenvalue problem can be formulated using the associated basis of Bloch functions,

$$|\boldsymbol{k}l\mu\sigma\rangle = \frac{1}{\sqrt{N_{\rm 2D}}}\sum_j e^{i\boldsymbol{k}\cdot\boldsymbol{R}_{lj}}|jl\mu\sigma\rangle, \tag{2}$$

constructed from the atomic orbitals $|lj\mu\sigma\rangle$, for each 2D wave vector $\boldsymbol{k}$ from the first 2D Brillouin zone (BZ). Here, $N_{\rm 2D}$ denotes the number of atoms in each atomic plane (with periodic boundary conditions at its edges) and it is equal to the number of $\boldsymbol{k}$ points in the BZ. In the Bloch representation, the matrix elements of the total Hamiltonian are diagonal in $\boldsymbol{k}$ and they are calculated as

$$\begin{aligned} H_{l'\mu'\sigma',l\mu\sigma}(\boldsymbol{k}) &= \langle\boldsymbol{k}l'\mu'\sigma'|H|\boldsymbol{k}l\mu\sigma\rangle \\ &= \sum_{j'} e^{-i\boldsymbol{k}\cdot(\boldsymbol{R}_{l'j'}-\boldsymbol{R}_{l0})}\langle l'j'\mu'\sigma'|H|l0\mu\sigma\rangle. \end{aligned} \tag{3}$$

The total Hamiltonian includes the one-electron SO interaction term [56,59]

$$H_{\rm SO} = \sum_{lj}\xi_l\,\boldsymbol{L}(\boldsymbol{r}-\boldsymbol{R}_{lj})\cdot\boldsymbol{S} \tag{4}$$

with matrix elements

$$\langle\boldsymbol{k}l'\mu'\sigma'|H_{\rm SO}|\boldsymbol{k}l\mu\sigma\rangle = \xi_l\langle\mu'\sigma'|\boldsymbol{L}\cdot\boldsymbol{S}|\mu\sigma\rangle\,\delta_{l'l}. \tag{5}$$

The SO coupling constant ξ_l corresponds to the metal forming the lth atomic layer in the investigated system. The values of the SO coupling for $3d$, $4d$, and $5d$ metals: $\xi_{\rm Fe} = 0.075$ eV, $\xi_{\rm Co} = 0.085$ eV, $\xi_{\rm Ni} = 0.105$ eV, $\xi_{\rm Cu} = 0.12$ eV, $\xi_{\rm Pd} = 0.23$ eV, $\xi_{\rm Ag} = 0.24$ eV, $\xi_{\rm Pt} = 0.65$ eV, and $\xi_{\rm Au} = 0.66$ eV are taken from Refs. [56,59,60]. The matrix elements of the operator $\boldsymbol{L}\cdot\boldsymbol{S}$ can be found, e.g., in Refs. [61,62].

The eigenstates, expanded as

$$|n\boldsymbol{k}\rangle = \sum_{l\mu\sigma} a^{\sigma}_{nl\mu}(\boldsymbol{k})|\boldsymbol{k}l\mu\sigma\rangle, \tag{6}$$

and their energies $\epsilon_n(\boldsymbol{k})$ are found from the $(18N)\times(18N)$ eigenvalue matrix equation

$$\sum_{l'\mu'\sigma'} H_{l\mu\sigma,l'\mu'\sigma'}(\boldsymbol{k})a^{\sigma'}_{nl'\mu'}(\boldsymbol{k}) = \epsilon_n(\boldsymbol{k})a^{\sigma}_{nl\mu}(\boldsymbol{k}). \tag{7}$$

Let us note that due to the presence of the SO interaction the eigenstates $|n\boldsymbol{k}\rangle$ of the Hamiltonian are *not* eigenstates of S_z. As a result the expansion (6) of $|n\boldsymbol{k}\rangle$ includes basis states of both spins $\sigma = \uparrow$ and $\sigma = \downarrow$.

C. Calculation of Gilbert damping

A quantum-mechanical expression for the Gilbert damping constant α has been derived by Kamberský in his torque correlation model [5,6]. An alternative derivation based on determining the damping part of the effective magnetic field

from the master equation for time-dependent electronic occupation factors is given in Ref. [63]. The formula for $\alpha = \omega_1/\omega_0$ can be also obtained by considering a long-wavelength spin wave with the frequency $\omega = \omega_0 + i\omega_1$, complex due to the SO coupling, in a similar way as it is done in Ref. [48] for the one-band model.

Kamberský's expression for the Gilbert damping constant reads

$$\alpha = \frac{\pi}{\mu_{\rm tot}} \int_{-\infty}^{\infty} d\epsilon\, \eta(\epsilon)\, {\rm tr}\{A^- L(\epsilon - H) A^+ L(\epsilon - H)\}, \quad (8)$$

where $\eta(\epsilon) = -df_{\rm FD}(\epsilon)/d\epsilon$ is the negative derivative of the Fermi-Dirac distribution function $f_{\rm FD}(\epsilon)$ and $\mu_{\rm tot}$ denotes the total spin magnetic moment in units of the Bohr magneton $\mu_{\rm B}$. The operator $A^- = [S^-, H_{\rm SO}]$ is the SO torque found with the spin lowering operator $S^- = S_x - iS_y$ (where $S_x = \frac{1}{2}\sigma_x$, $S_y = \frac{1}{2}\sigma_y$ are defined with the Pauli matrices σ_x, σ_y), A^+ is its Hermitian conjugate, and $L(\epsilon - H)$ stands for the Lorentz function defined as $L(x) = (\Gamma/2\pi)/(x^2 + \Gamma^2/4)$ where Γ is the electron-scattering rate.

The general formula (8) can be employed to calculate the Gilbert damping constant α in various magnetic systems. For a magnetic layered system with one ferromagnetic layer the following expression for the Gilbert damping constant is found:

$$\alpha = \frac{\pi}{N_{\rm FM}\mu_{\rm s}} \sum_{n,n'} \frac{1}{\Omega_{\rm BZ}} \int d\boldsymbol{k} |A_{nn'}(\boldsymbol{k})|^2 F_{nn'}(\boldsymbol{k}), \quad (9)$$

based on the matrix $A_{nn'}(\boldsymbol{k})$ elements and the energy factor $F_{nn'}(\boldsymbol{k})$ defined below. Here the integration over $\boldsymbol{k} = (k_x, k_y)$ is done over the 2D BZ, $\Omega_{\rm BZ}$ is the volume of the BZ, $\mu_{\rm s}$ denotes the atomic magnetic moment (in units of $\mu_{\rm B}$) of the ferromagnet, and $N_{\rm FM}$ stands for the number of atomic layers in the ferromagnetic part of the system. For a film with fcc structure and the lattice constant a, $\Omega_{\rm BZ}$ is equal to $(2\pi/a_{2d})^2$ where $a_{2d} = a/\sqrt{2}$ is the (001) fcc surface square lattice constant.

The matrix elements

$$A_{nn'}(\boldsymbol{k}) = \langle n\boldsymbol{k}|A^-|n'\boldsymbol{k}\rangle = \langle n\boldsymbol{k}|[S^-, H_{\rm SO}]|n'\boldsymbol{k}\rangle \quad (10)$$

are calculated as

$$A_{nn'}(\boldsymbol{k}) = \sum_{l,\mu\sigma,\mu'\sigma'} \xi_l\, a^{\sigma}_{nl\mu}(\boldsymbol{k})^*\, a^{\sigma'}_{n'l\mu'}(\boldsymbol{k}) \langle \mu\sigma|A^-_{\rm at}|\mu'\sigma'\rangle, \quad (11)$$

where

$$A^-_{\rm at} = [S^-, \boldsymbol{L}\cdot\boldsymbol{S}] = L_z S^- - L^- S_z \quad (12)$$

is the SO torque coming from a single atom with a unit SO coupling constant. The matrix elements of this torque can be found using the elements of the SO coupling,

$$\langle \mu\uparrow|A^-_{\rm at}|\mu'\uparrow\rangle = -\langle \mu\uparrow|\boldsymbol{L}\cdot\boldsymbol{S}|\mu'\downarrow\rangle, \quad (13a)$$

$$\langle \mu\uparrow|A^-_{\rm at}|\mu'\downarrow\rangle = 0, \quad (13b)$$

$$\langle \mu\downarrow|A^-_{\rm at}|\mu'\uparrow\rangle = 2\langle \mu\uparrow|\boldsymbol{L}\cdot\boldsymbol{S}\,|\mu'\uparrow\rangle, \quad (13c)$$

$$\langle \mu\downarrow|A^-_{\rm at}|\mu'\downarrow\rangle = -\langle \mu\uparrow|A^-_{\rm at}|\mu'\uparrow\rangle. \quad (13d)$$

These elements vanish for the same spin orbitals $(\mu\sigma) = (\mu'\sigma')$ as well as for orbitals μ and μ' with different orbital numbers, regardless of their spins σ, σ', since the corresponding matrix elements of $\boldsymbol{L}\cdot\boldsymbol{S}$ also vanish [61,62].

The factor $F_{nn'}(\boldsymbol{k})$ is defined by integrating the product of $\eta(\epsilon) = -df_{\rm FD}/d\epsilon$, dependent on temperature T, and the two Lorentzians depending on eigenenergies $\epsilon_n(\boldsymbol{k})$, $\epsilon_{n'}(\boldsymbol{k})$ (with band indexes n, n'),

$$F_{nn'}(\boldsymbol{k}) = \int_{-\infty}^{\infty} d\epsilon\, \eta(\epsilon) L[\epsilon - \epsilon_n(\boldsymbol{k})] L[\epsilon - \epsilon_{n'}(\boldsymbol{k})]. \quad (14)$$

At $T = 0$, this factor becomes $L[\epsilon_{\rm F} - \epsilon_n(\boldsymbol{k})]L[\epsilon_{\rm F} - \epsilon_{n'}(\boldsymbol{k})]$ where $\epsilon_{\rm F}$ is the Fermi energy.

It is noteworthy that the explicit temperature dependence of the Gilbert damping appears solely in Eq. (14): in the derivative $\eta(\epsilon)$ of the distribution function $f_{\rm FD}(\epsilon)$. The damping is also physically altered by temperature via the electron-scattering mechanism due to lattice vibrations but the corresponding average scattering rate Γ is treated here as an independent parameter.

The presence of $\eta(\epsilon)$ in Eq. (14) makes the Gilbert damping be affected predominantly by states with energies close to the Fermi level $\epsilon_{\rm F}$. Contributions to the Gilbert damping constant given by Eq. (9) can be attributed to two kinds of electronic transitions invoked by the SO coupling: intraband ($n = n'$) and interband ($n \neq n'$). The former indicate transitions within a single energy band and gives contributions to the conductivitylike terms of damping, while the latter, corresponding to transitions between different energy bands, give the resistivitylike terms of damping as already discussed in Refs. [5] and [63] in detail.

The obtained expression for the Gilbert damping constant within the TB model can be employed to calculate this constant in a variety of layered magnetic structures (with a straightforward modification to the total magnetic moment $N_{\rm FM}\mu_s$ needed in the case where more than one FM layer is present in a given system). In the present study, the damping constant is calculated for FM films and Co/NM bilayers as well as bulk ferromagnetic metals. The calculations are done for a wide range of electron-scattering rates Γ (expressed as $\hbar/\tau$ with the lifetime τ in Ref. [39]): $0.001\ {\rm eV} \leqslant \Gamma \leqslant 2.0\ {\rm eV}$.

The energy bands $\epsilon_n(\boldsymbol{k})$ and states $|n\boldsymbol{k}\rangle$ used in the calculation of the damping constant α with Eqs. (9)–(14) are found with the Hamiltonian including the SO interaction $H_{\rm SO}$. The inclusion of the SO coupling term in the Hamiltonian is found to be essential for the intraband terms ($n = n'$) and gives a significant contribution to the Gilbert damping constant α.

To illustrate this fact, in Fig. 1 we plot α in bulk Fe and Co for two different cases: with and without the SO interaction in the calculation of electronic band structure. This distinction refers only to states $|n\boldsymbol{k}\rangle$ and energies $\epsilon_n(\boldsymbol{k})$. In both cases the same full SO coupling is kept in the SO torque A^-. Thus, it is found that including the SO interaction $H_{\rm SO}$ in the Hamiltonian is crucial for reproducing a qualitatively correct dependence of α on the scattering rate Γ, especially in the range of small $\Gamma < 0.05$ eV for which the intraband term dominates; see Fig. 1. A very similar conclusion based on results for bulk Fe has been previously reported in Ref. [6].

These results can be explained by noting that the intraband terms $A_{nn}(\boldsymbol{k})$ vanish if the SO coupling is neglected in the energy-band calculation for cubic ferromagnets as well as for layered systems with the inversion symmetry. Indeed, in the

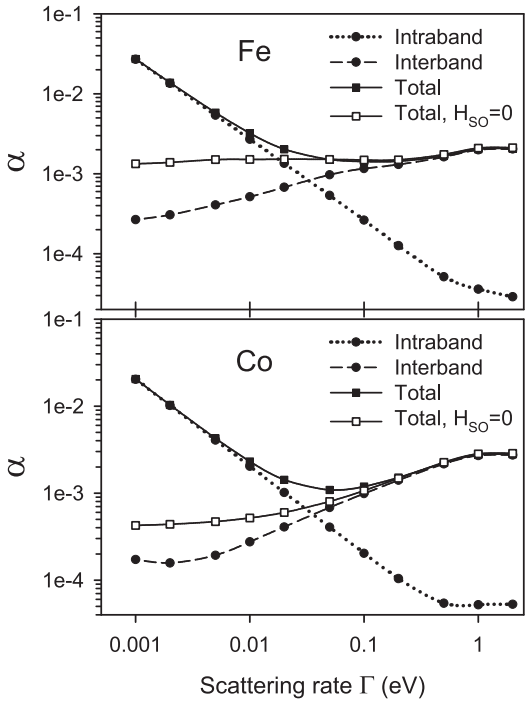

FIG. 1. Gilbert damping constant α (solid lines) and its intraband (dotted line) and interband (dashed line) terms vs scattering rate Γ for bulk Fe and Co found with (solid symbols) and without (open squares) the SO interaction $H_{\rm SO}$ in the band structure calculation.

absence of $H_{\rm SO}$ the states $|n\boldsymbol{k}\rangle$ become the eigenstates $|n_0\sigma\boldsymbol{k}\rangle$ of S_z so that the resultant matrix elements

$$\begin{aligned} A_{nn}(\boldsymbol{k}) &= \sum_{lj} \xi_l \langle n_0\sigma\boldsymbol{k}|L_z(\boldsymbol{r}-\boldsymbol{R}_{lj})S^- - L^-(\boldsymbol{r}-\boldsymbol{R}_{lj})S_z|n_0\sigma\boldsymbol{k}\rangle \\ &= -\frac{1}{2}s_\sigma \sum_{lj} \xi_l \langle n_0\sigma\boldsymbol{k}|L^-(\boldsymbol{r}-\boldsymbol{R}_{lj})|n_0\sigma\boldsymbol{k}\rangle \\ &= -\frac{1}{2}s_\sigma \langle n_0\sigma\boldsymbol{k}|O^-(\boldsymbol{r})|n_0\sigma\boldsymbol{k}\rangle \end{aligned} \tag{15}$$

(where $s_\uparrow = 1$, $s_\downarrow = -1$, and $O^- = O_x + iO_y$) vanish for any nondegenerate state $|n_0\sigma\boldsymbol{k}\rangle$ due to quenching of the orbital angular momentum. To show this let us note that the operator $O_\zeta(\boldsymbol{r}) = \sum_{lj} \xi_l L_\zeta(\boldsymbol{r}-\boldsymbol{R}_{lj})$ $(\zeta = x,y,z)$ becomes $[O_\zeta(-\boldsymbol{r})]^* = -O_\zeta(\boldsymbol{r})$ under the combined action of the complex conjugation and the inversion operator $\boldsymbol{r} \to -\boldsymbol{r}$ while the nondegenerate states $|n_0\sigma\boldsymbol{k}\rangle$ remain unchanged up to a constant phase factor $e^{i\varphi}$; see Appendix in Ref. [59]. The contribution of degenerate states is negligible since they correspond to a set of $\boldsymbol{k}$ points with zero measure.

It is interesting to note that the perturbation theory for nondegenerate states seemingly fails to reproduce the correct ξ^3 dependence of the intraband term $\alpha_{\rm intra}$ on the SO coupling constant ξ in bulk ferromagnets, found in previous calculations, e.g., in Ref. [63]. Indeed, the first-order expansion $|n\boldsymbol{k}\rangle = |n_0\sigma\boldsymbol{k}\rangle + |n\boldsymbol{k}\rangle^{(1)}$ with $|n\boldsymbol{k}\rangle^{(1)} \sim \xi$ leads to the relation $A_{nn'}(\boldsymbol{k}) \sim \xi^2$ and consequently to $\alpha_{\rm intra} \sim \xi^4$. The ξ^3 dependence of $\alpha_{\rm intra}$ is retained if the perturbation theory for nearly degenerate states is applied as it has already been shown for bulk metals in the original work by Kamberský [5]. Therein, the contribution to $\alpha_{\rm intra}$ proportional to ξ^3 is shown to come from a finite area of the Fermi surface (FS) (or rather, for $T > 0$, a finite slice of the BZ including this part of the FS). This area includes the $\boldsymbol{k}$ points forming a striplike region on the FS around the line where two different energy bands cross each other at the FS in the absence of $H_{\rm SO}$. The strip width is proportional to ξ since the states from two bands can be considered as nearly degenerate as long as their energy separation is of the order of ξ. Then, the perturbed states are well approximated by combinations of the two unperturbed states only so that the corresponding matrix elements $A_{nn}(\boldsymbol{k})$ do not vanish for the perturbed states. Since $A_{nn}(\boldsymbol{k})$ are proportional to ξ the contribution to $\alpha_{\rm intra}$ coming from the striplike region in the BZ is proportional to ξ^3. Let us also note that the interband term of the damping constant α depends quadratically on the SO coupling constant ξ [63].

D. Numerical efficiency and convergence of Gilbert damping calculation

The factor $F_{nn'}(\boldsymbol{k})$ dependent on the energies $\epsilon_n(\boldsymbol{k})$ and $\epsilon_{n'}(\boldsymbol{k})$ can be calculated directly according to its definition given in Eq. (14) as it has been presumably done in previous calculations, e.g., Ref. [39]. However, the involved energy integral must be computed with suitable care to get accurate results due to the rapid variation of both the two Lorentzian functions as well as the negative derivative $\eta(\epsilon)$ of the Fermi-Dirac function. Instead of using numerical integration, the factor $F_{nn'}(\boldsymbol{k})$ can be determined more efficiently by replacing the integral by the sum of the residues of the integrand. Additionally, better control of the numerical accuracy is achieved by including in this sum a sufficient number of the Matsubara frequencies (around 40 of them have been found to be sufficient for $T = 300$ K). The detailed analytical expression for $F_{nn'}(\boldsymbol{k})$ is derived in the Appendix.

The convergence of the Gilbert damping constant with number of $\boldsymbol{k}$ points in the BZ is investigated for bulk bcc Fe and fcc Co as well as (001) fcc Co(5 ML) and Co(20 ML) films with different values of the scattering rate Γ. The results shown in Figs. 2 and 3 clearly show the advantage of using finite T since much smaller number of $\boldsymbol{k}$ points is needed for the convergence of α than at $T = 0$.

For bulk ferromagnets (Fig. 2) it is found that using $T = 300$ K the convergence of α is reached with as few as 100^3 $\boldsymbol{k}$ points (for $\Gamma \geqslant 0.001$ eV) while one may need as many as 300^3 and 600^3 $\boldsymbol{k}$ points, to attain convergence for $\Gamma = 0.01$ eV and $\Gamma = 0.001$ eV, respectively, at $T = 0$. A similar number of $\boldsymbol{k}$ points, 100^3 or slightly more, has been used in previously reported *ab initio* calculations for bulk systems at finite temperature where α is given by Eqs. (9) and (14).

In the case of the layered systems with $\Gamma \geqslant 0.01$ eV we obtain convergence with 100^2 $\boldsymbol{k}$ points at $T = 300$ K while more than 400^2 $\boldsymbol{k}$ points may be needed at $T = 0$. The number of $\boldsymbol{k}$ points required for convergence increases for smaller Γ and varies with the film thickness. For the smallest scattering rate $\Gamma = 0.001$ eV, around 1000^2 $\boldsymbol{k}$ points are needed to give a satisfactory convergence of α calculated at $T = 300$ K while even using 2000^2 $\boldsymbol{k}$ points do not lead to a convergent result for $T = 0$.

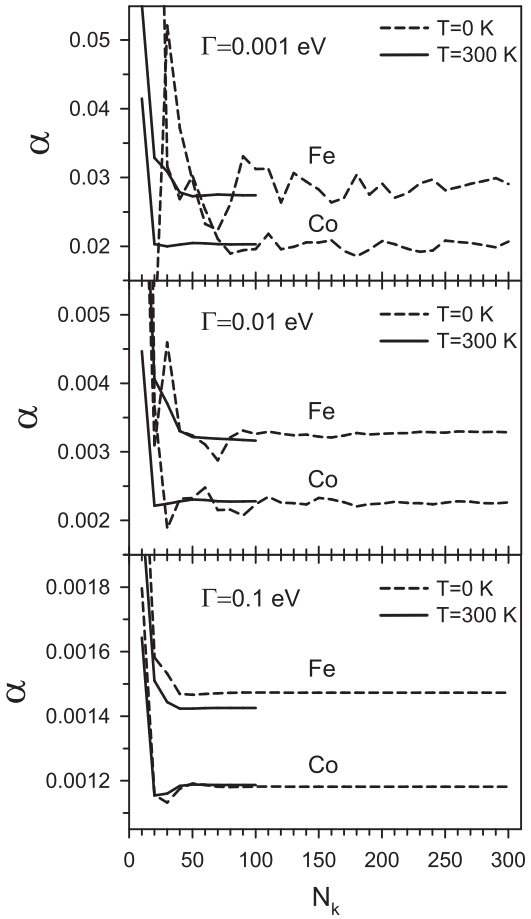

FIG. 2. Convergence of the Gilbert damping constant α with the number $(2N_k + 1)^3$ $\boldsymbol{k}$ points in the 3D BZ for bulk Fe and Co at $T = 0$ (dashed lines) and $T = 300$ K (solid lines), for different scattering rates Γ.

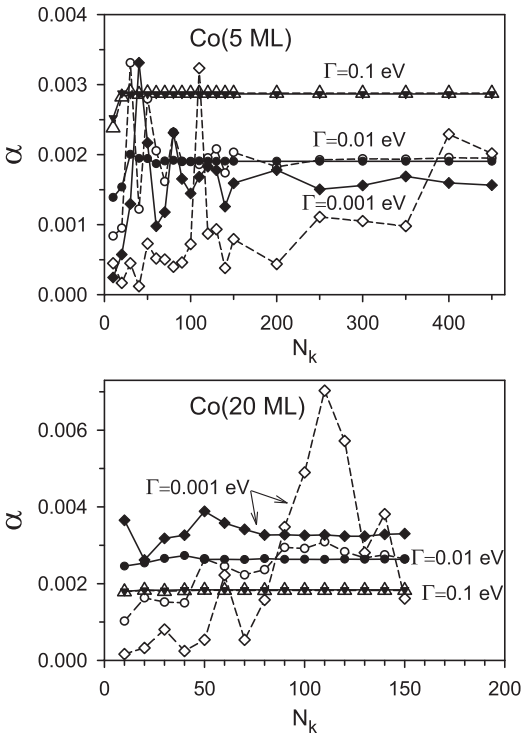

FIG. 3. Convergence of the Gilbert damping constant α with the number $(2N_k + 1)^2$ $\boldsymbol{k}$ points in the 2D BZ for (001) fcc Co(5 ML) and Co(20 ML) films at $T = 0$ (open symbols, dashed lines) and $T = 300$ K (solid symbols and lines), for different scattering rates: $\Gamma = 0.001$ eV (diamonds), $\Gamma = 0.01$ eV (circles), and $\Gamma = 0.1$ eV (triangles).

Furthermore, the calculations done for various temperatures $0 \leqslant T \leqslant 600$ K have shown that the Gilbert damping constant is weakly dependent on temperature which confirms the previous findings [39]. Indeed, the damping constants α calculated for ferromagnetic bulk metals and films at zero and finite T ultimately saturate to very similar values as the number of $\boldsymbol{k}$ points increases. In particular, we find that in Co(5 ML) and Co(10 ML) films the converged value of α is almost the same at $T = 0$ and $T = 300$ K for $\Gamma \geqslant 0.01$ eV, a significant discrepancy being obtained only for $\Gamma < 0.01$ eV; see Fig. 4. Thus, using finite temperature is found to improve efficiency of numerical calculations while hardly affecting the actual results for the damping constant except for very small scattering rates Γ.

The numerical efficiency of the Gilbert damping calculations is also improved by limiting the integration over $\boldsymbol{k}$ in Eq. (9) to the irreducible BZ, which is the 1/8 BZ in the case of layered systems with the cubic symmetry. It has been checked in numerical tests for each investigated system that the values of α obtained by integrating over the 1/8 BZ are identical to the results of the integration over the full BZ. It is expected that this equality results from the invariance of the Hamiltonian H under the time-reversal and spatial symmetry operations.

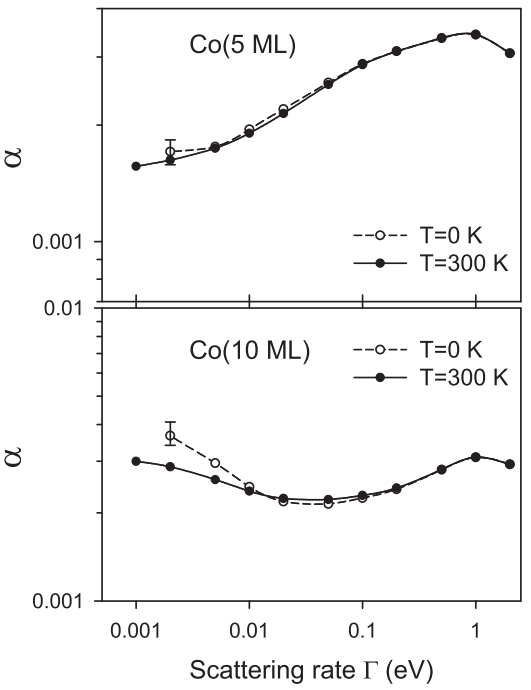

FIG. 4. Gilbert damping constant α vs the scattering rate Γ in (001) fcc Co(5 ML) and Co(10 ML) films at $T = 0$ and $T = 300$ K. Open symbols show damping at $T = 0$ and the solid ones stand for $T = 300$ K. The error bars shown for $\Gamma = 0.002$ eV at $T = 0$ reflect the not fully converged summation over the BZ with $N_k = 1000$ for Co(5 ML) and $N_k = 700$ for Co(10 ML).

III. RESULTS

A. Ferromagnetic films

The Gilbert damping constant α calculated for bcc Fe, fcc Co, and fcc Ni ferromagnetic films with (001) surface is found to be considerably changed in comparison with the respective bulk ferromagnets [43]. Both significant enhancement and large reduction of α are obtained depending on the scattering rate Γ and the investigated metal as well as the film thickness; see Fig. 5. The largest changes in the magnetic damping occur for films of a few monolayers thickness and the smallest investigated scattering rates. For $\Gamma = 0.001$ eV there is an over tenfold decrease of α for 5-ML films of Fe and Co and an over 50-fold decrease for the 5-ML Ni film. The Gilbert damping α is enhanced for Co films with $0.02\ \text{eV} \leqslant \Gamma \leqslant 1$ eV and for Fe films thicker than 9 ML in the entire investigated range of Γ, especially, for $\Gamma \leqslant 0.5$ eV. For ultrathin Fe films of a few ML thickness, the enhancement of α is limited to some intermediate range of investigated scattering rate (e.g., $0.02\ \text{eV} \leqslant \Gamma \leqslant 1$ eV for $N = 5$) while the aforementioned decrease of α is found for smaller Γ. In the case of Ni films the obtained α is largely reduced in comparison with bulk Ni for $\Gamma \leqslant 0.02$ eV. For large scattering rates ($\Gamma \geqslant 1$ eV for Fe and Co, and $\Gamma \geqslant 0.1$ eV for Ni) the damping constant α for thin films is close to the bulk value. As a general trend, we find that the values of α calculated for ferromagnetic films tend to the corresponding bulk value with increasing film thickness for the majority of the assumed scattering rates $0.001\ \text{eV} \leqslant \Gamma \leqslant 2$ eV. However, the convergence to the bulk value is slow in most cases, as seen in Fig. 6.

The dependence of the damping constant α on the film thickness for ferromagnetic bcc Fe, fcc Co, and fcc Ni films with two different scattering rates is shown in Fig. 6. The characteristic oscillations of damping with film thickness are obtained for all three metals and they are attributed to quantum well (QW) states with energies at the Fermi level. This interpretation is supported by the fact that the obtained oscillations have a smaller amplitude for larger Γ. Indeed, this can be explained by larger smearing of the electronic energy levels (and the energies of QW states, in particular) described by the Lorentz function. The occurrence of QW states in metallic films is a well-known phenomenon which also leads to oscillations of interlayer exchange coupling and magnetic anisotropy with varying thicknesses of ferromagnetic films and/or nonmagnetic layers [58,59,64–72]. Further discussion

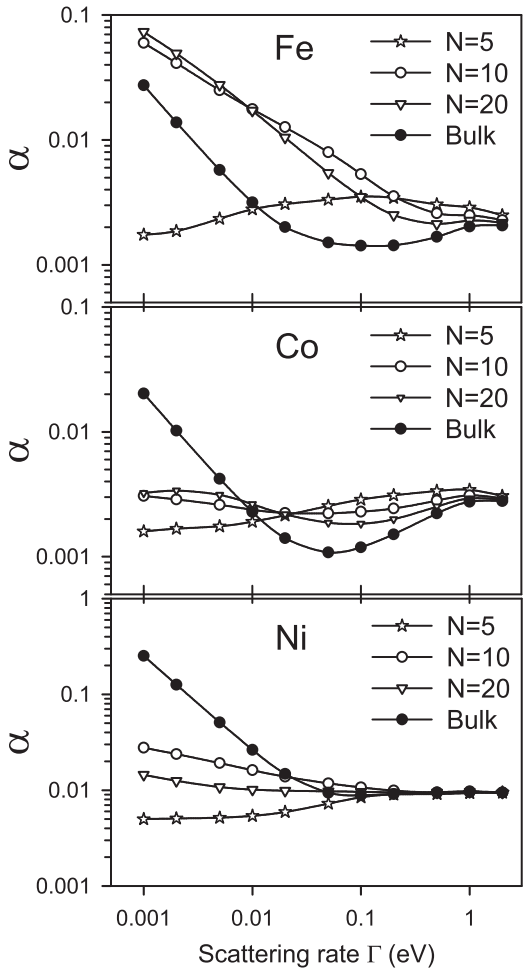

FIG. 5. Gilbert damping constant α vs scattering rate Γ in bulk ferromagnets (bcc Fe, fcc Co, fcc Ni) and (001) ferromagnetic films with different thicknesses N.

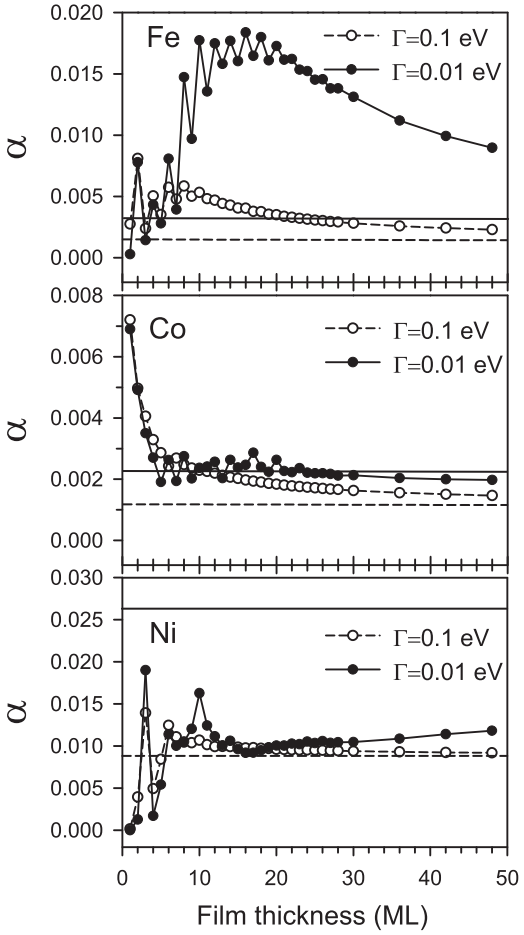

FIG. 6. Gilbert damping constant α vs film thickness for (001) bcc Fe, fcc Co, and fcc Ni films, calculated with the scattering rates $\Gamma = 0.01$ eV and $\Gamma = 0.1$ eV, $T = 300$ K. The horizontal lines mark the bulk values of α for $\Gamma = 0.1$ eV (dashed line) and $\Gamma = 0.01$ eV (solid line).

on the Gilbert damping oscillations is given below in this section.

For bcc Fe films, the plot of α against film thickness has a broad maximum at the thickness of several ML (at 16 ML for $\Gamma = 0.01$ eV, and at the lower thickness of 7 ML for a larger scattering rate of $\Gamma = 0.1$ eV) and shows a slow decay of α for larger thicknesses. As a result, the damping constant α for both scattering rates is still far from the corresponding bulk values even for the thickest investigated film thickness of $N = 48$ ML.

For fcc Co films, the damping constant α decreases as the film thickness increases, with small QW states oscillations superimposed on this monotonic dependence. If these small oscillations are neglected, α is found to saturate at the bulk value of 0.0023 for $\Gamma = 0.01$ eV, already at $N = 10$ ML, and to approach closely the bulk value of 0.0012 for $\Gamma = 0.1$ eV at a Co thickness of $N \approx 40$ ML.

In the case of fcc Ni films, an increasing trend is obtained in the overall dependence of the calculated α on the increasing film thickness. However, large oscillations of α due to QW states in Ni films disturb this trend more strongly, especially for $N \leqslant 12$ ML, than oscillations due to QW states in Fe and Co films. The Gilbert damping constant for Ni films with $\Gamma = 0.1$ eV saturates at the bulk value at $N \approx 20$ ML. For smaller scattering rate of $\Gamma = 0.01$ eV, the damping constant seemingly starts to saturate at $N \approx 25$ ML. However, this trend is deceptive since α is only a third of its calculated bulk value (0.026) at $N = 25$ ML and for the Ni thickness larger than 30 ML the damping constant increases monotonically up to the largest investigated thickness of $N = 48$ ML. Thus, it is expected that for $\Gamma = 0.01$ eV the actual convergence of α to the bulk Ni value will take place at much larger film thicknesses, presumably around 300 ML as can be estimated by extrapolating the monotonic dependence seen for $N > 30$ ML in Fig. 6.

The results obtained for ferromagnetic films imply that the damping constant can be enhanced several times in comparison to bulk metals. The maximum enhancement for $\Gamma = 0.01$ eV is found for the 16-ML Fe film (5.5 times) and the Co monolayer (over threefold). In the case of Ni films a significant enhancement [nearly 67% for Ni(3 ML) with $\Gamma = 0.05$ eV] occurs merely for larger scattering rates ($0.02\,\text{eV} \leqslant \Gamma \leqslant 0.2\,\text{eV}$). Simultaneously, a large reduction of α (over tenfold) is obtained for Fe and Ni films of a few ML thickness, in particular for $N = 1,3$ ML for Fe and $N = 1,2,4$ ML for Ni. The obtained enhancement oscillates with the film thicknesses and it decays for thicker films as the damping constant approaches the bulk limit. The enhancement of the Gilbert damping (or, more generally, its modification) in free-standing thin ferromagnetic films, in comparison to bulk metals, is related to the change of the electronic structure due to the loss of 3D translational symmetry. In particular, this change results in the quantization of the wave vector in the direction perpendicular to the film surface and the subsequent occurrence of the QW states which in turn leads to oscillations of the damping constant with increasing film thickness.

The obtained oscillatory dependence of the damping constant on the film thicknesses has a different character for different metals. While only one clear period of 2 ML is present for the Fe films, the identification of similar periods for Co and Ni films is not straightforward, with two different periods being possible (e.g., ~3.5 ML and ~7 ML for Ni); cf. Fig. 6. The oscillation periods associated with QW states are related to the extremal radii of Fermi-surface sheets of the corresponding bulk metals. However, it remains to be investigated which points or regions in the 2D BZ are responsible for the occurrence of the QW states contributing to the Gilbert damping oscillations. This question is valid in particular in view of the earlier theoretical predictions [58,59,66], recently confirmed experimentally [71,72], that the magnetic anisotropy energy (also related to the SO coupling) of (001) fcc Co film oscillates with one clear period close to 2 ML. These oscillations have been shown [58] to come from the center of the 2D BZ where there are pairs of QW states degenerate at the $\overline{\Gamma}$ point.

The oscillatory behavior of the Gilbert damping constant is found to originate mainly from the interband term, so that the obtained oscillations come from pairs of QW states with energies close to each other as well as to the Fermi level ϵ_F. Thus, we conclude that the oscillations of the Gilbert damping arise due to a similar mechanism as magnetocrystalline anisotropy (MA) oscillations which have been shown to come from pairs of QW states, one state lying below ϵ_F and the other above ϵ_F [58,67,68]. However, the important difference is that the states significantly contributing to the Gilbert damping lie within a few Γ off the Fermi level ϵ_F, due to the presence of the product $L[\epsilon - \epsilon_n(\boldsymbol{k})]L[\epsilon - \epsilon_{n'}(\boldsymbol{k})]$ in Eq. (14). In the case of MA the energy range of the contributing states is much wider as the suppressing factor $1/[\epsilon_n(\boldsymbol{k}) - \epsilon_{n'}(\boldsymbol{k})]$ present in the second-order perturbation theory expression for the MA energy [59] does not decay so rapidly as the energies, $\epsilon_n(\boldsymbol{k})$ and/or $\epsilon_{n'}(\boldsymbol{k})$, move away from ϵ_F. As a result of this difference the regions in the $\boldsymbol{k}$ space that give dominating contributions to the magnetic damping are much more restricted than for the MA. This conclusion should also hold for contributions from the QW states.

Another important difference between the MA energy and the Gilbert damping constant α is the different operators involved in the calculation of the two quantities. These operators are the SO interaction H_{SO} (for two separate orientations of magnetization) in the former case, and the SO torque A^- in the latter. Thus, a particular pair of QW states can contribute to the MA energy and the Gilbert damping in a significantly different way, or even not contribute at all for one of them, due to specific spatial and spin symmetry of the corresponding operators. In conclusion, a further study is needed to explain the origin of the Gilbert damping oscillations, in particular, the responsible QW states and the associated oscillation periods.

Figure 7 depicts α against film thickness at two different temperatures ($T = 0$ and $T = 300$ K) in Co films. As is seen, the change of α due to change of temperature is not significant and for most thicknesses α is almost the same at both $T = 0$ and $T = 300$ K, although the oscillations of α with changing Co film thickness have a larger amplitude at $T = 0$ due to the lack of smearing of energy levels. A similar conclusion was previously found to hold for magnetic anisotropy energy and its oscillations in Co films [59].

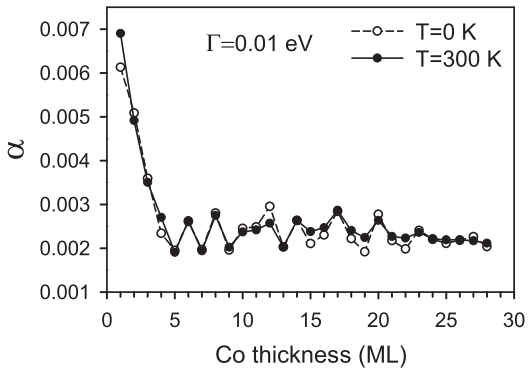

FIG. 7. Gilbert damping constant α vs film thickness at $T = 0$ and $T = 300$ K in (001) fcc Co films; $\Gamma = 0.01$ eV.

B. Ferromagnet/nonmagnet bilayers

In this section, we report on the results of TB calculations of the Gilbert damping constant α in (001) fcc cobalt/nonmagnet (Co/NM) bilayers with Co as a ferromagnetic substrate and various nonmagnetic caps: NM = Cu, Pd, Ag, Pt, and Au. The dependence of α on both the Co and NM thicknesses, $N_{\mathrm{FM}} = N_{\mathrm{Co}}$ and N_{NM}, is investigated. The damping constant is calculated with Eqs. (9)–(14) using the eigenvalues and eigenstates found in the way explained in Sec. II B. The expression for the damping constant α in bilayer systems depends on the SO coupling constants of both ferromagnetic and nonmagnetic metals.

It is found that the Gilbert damping is remarkably enhanced in the investigated Co/NM(6 ML) bilayers, particularly strongly for very small Co thickness; see Fig. 8. The presence of the NM caps makes the damping constant α about an order of magnitude larger than in pure Co films, and even a few times more in the case of the Pt cap. The enhancement of α in Co/NM bilayers becomes weaker for thicker Co films and the dependence of α on the Co thickness N_{Co} shows a monotonic decrease with increasing N_{Co}. The damping constant of Co/NM(6 ML) bilayers decreases by more than an order of magnitude (about 27 times for Cu, 22 times for Ag, 42 times for Pd, 45 times for Pt, and 47 times for Au caps) as the Co thickness increases from 1 to 28 ML. A similar

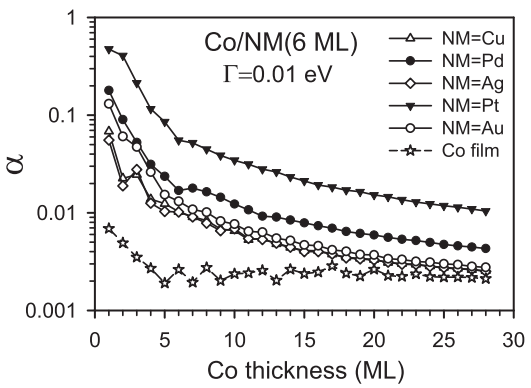

FIG. 8. Gilbert damping constant vs Co thickness in (001) fcc Co/NM(6 ML) bilayers; $\Gamma = 0.01$ eV.

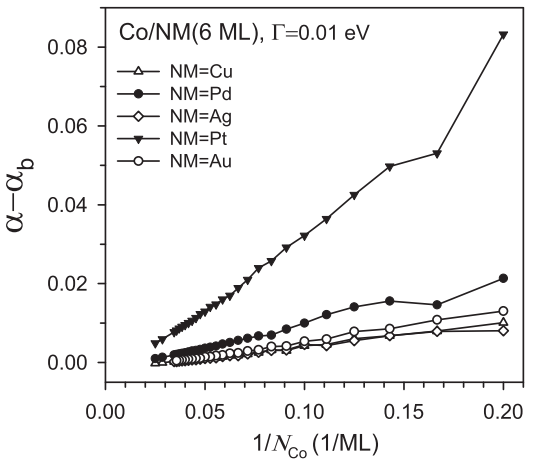

FIG. 9. Inverse Co thickness dependence of the additional damping in (001) fcc Co/NM(6 ML) bilayers due to adding the NM caps; $\Gamma = 0.01$ eV.

dependence of α on the Co thicknesses is obtained for Co/NM bilayers with the NM cap of other thicknesses, even just 2 ML.

The results obtained for Co/NM bilayers satisfy the following approximate relation:

$$\alpha \approx \alpha_{\mathrm{b}} + \alpha_{\mathrm{s}}/N_{\mathrm{FM}}. \tag{16}$$

This linear dependence on $1/N_{\mathrm{FM}}$ ($= 1/N_{\mathrm{Co}}$ herein) is demonstrated in Fig. 9 where the additional damping (enhancement) $\alpha - \alpha_{\mathrm{b}}$ due to adding the NM caps only is shown. Equation (16) simply implies that the total damping constant α in Co/NM bilayers, redefined as the extensive quantity $\tilde{\alpha} = N_{\mathrm{FM}}\alpha$, consists of the bulklike contribution $N_{\mathrm{FM}}\alpha_{\mathrm{b}}$ from the ferromagnet and the additional term α_{s} responsible for the enhancement. The latter term is the combined contributions coming from the FM/vacuum and FM/NM interfaces present in the system, as well as, in the case of NM = Pd and Pt, from several atomic layers inside the NM cap close to the FM/NM interface; see Sec. III C. Thus, the equation (16) presents a direct connection between the film and bulk regime.

A similar monotonic dependence on $1/N_{\mathrm{FM}}$, though following a sublinear power law, is found in Ref. [9] for the ratio $\Delta\omega/\omega_0$ of the linewidth $\Delta\omega$ and the frequency ω_0 of a long-wavelength spin wave in an (001) Co/Pd bilayer. If the usual definition of $\Delta\omega$ as the full width at half maximum is adopted (though not stated explicitly in Refs. [8,9]) the linewidth $\Delta\omega$ is twice the imaginary part ω_1 of the complex spin-wave frequency $\omega = \omega_0 + i\omega_1$. Then, the damping constant α obtained for Co/Pd bilayer (Fig. 8) is around two or three times larger than the values of $\alpha = \omega_1/\omega_0 = 0.5\Delta\omega/\omega_0$ reported in Ref. [9]. However, it should be noted that the two methods of calculating α are significantly different since the cited calculations of the spin-wave spectrum do not account for the lifetime $\tau = 1/\Gamma$ of electronic states due to electron-phonon scattering.

Recently, a linear dependence of α on $1/N_{\mathrm{Co}}$ has been found experimentally in Pt/Co/Pt trilayers. [22] A similar linear dependence of the magnetic damping constant on the inverse of the ferromagnetic film thickness in Eq. (16) has also been observed in experiments on ultrathin bcc Fe(001) films

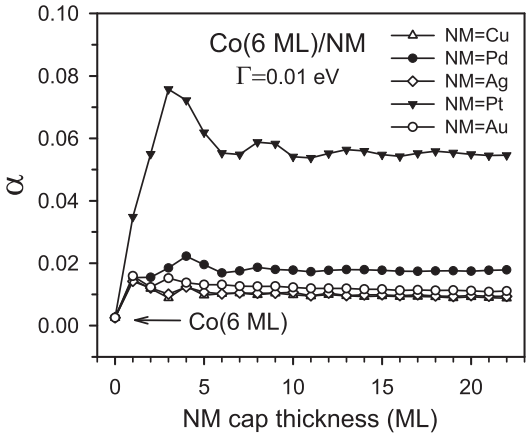

FIG. 10. Gilbert damping constant vs NM cap thickness in (001) fcc Co(6 ML)/NM bilayers; $\Gamma = 0.01$ eV.

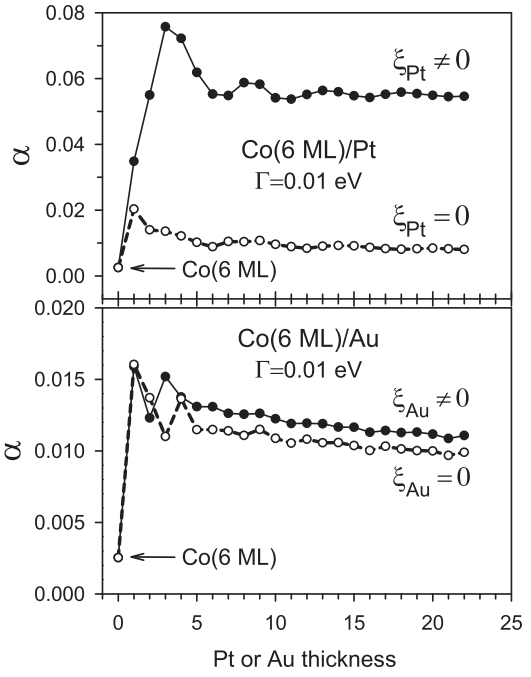

FIG. 11. Gilbert damping constant vs NM cap thickness in (001) fcc Co(6 ML)/NM bilayer (NM = Pt and Au), in the presence (solid circles) and the absence (open circles) of the SO coupling in NM; $\Gamma = 0.01$ eV.

grown on Ag(001) [15,16] and Ni-based bilayers [25] as well as CoFeB [26] and Fe/Au films. [19] In these experiments the FMR linewidth and its term proportional to α have been determined.

In Fig. 10 we present α as a function of the NM cap thickness in Co(6 ML)/NM bilayers. For comparison, the value of α for the Co(6 ML) film ($\alpha = 0.0026$ for $\Gamma = 0.01$ eV) is also marked in the plot. The enhancement of the Gilbert damping is obtained even for the thinnest NM overlayers, 1 or 2 ML thick. For NM = Pd and Pt caps, there is a large initial increase of damping for the cap thicknesses extending up to 4 ML which is followed by an oscillatory dependence for larger cap thicknesses. Such oscillatory dependence on the NM cap thickness is present for all investigated bilayers though it is not well visible in Fig. 10 due to the figure scale. We attribute these oscillations, with the amplitude decreasing with the increase of the cap thickness, to the QW states present in the NM metal. The oscillation periods can be related to extremal radii of the FS of the bulk nonmagnets. In the case of Pd and Pt, the sheet of the FS coming from the bulk d band of the Δ_5 symmetry yields the period of 5.7 ML [73]. This oscillation period has previously been found for the MA energy in Co/Pd systems [67,68]. A similar, though slightly shorter, period of around 5 ML is presently found in the dependence of the damping constant on the Pd and Pt cap thicknesses; see Fig. 10.

The obtained enhancement of the Gilbert damping in Co/NM bilayers results from two main factors: (i) strong SO coupling in nonmagnetic elements heavier than Co, (ii) change of electronic structure due to hybridization at the Co/NM interface. The former directly appears in the expression for α, namely in Eq. (11), while both factors affect damping through the modification of the electronic states and their energies which enter Eqs. (11) and (14).

To investigate the role of the two factors and their possible interplay we compare the damping constants calculated for the Co/Pt and Co/Au bilayers with zero and full SO coupling in the NM cap; see Fig. 11. It is found that, although the two NM metals, Pt and Au, have very similar SO coupling constants, around 8.5 times larger than Co, switching on this coupling has a diametrically different effect on α in the two bilayer systems. While the results for the Co/Au bilayer obtained with $\xi_{Au} =$ 0 and $\xi_{Au} = 0.66$ eV differ by less than 15%, the damping constant for the Co/Pt bilayer increases over fivefold if $\xi_{Pt} = 0.65$ eV is used instead of $\xi_{Pt} = 0$. Thus we find that the Gilbert damping depends strongly on the SO coupling of the Pt cap and only slightly on the SO coupling of the Au cap. This remarkably different dependence of α on ξ_{NM} is due to the presence of d states at the Fermi level ϵ_F in Pt and the lack of such states in Au. To explain this relationship let us recall that the structure for the expression for α strongly favors quantum states with energies in the immediate vicinity of ϵ_F [due to the form of the integrand in Eq. (14)]. Because of the different energetic positions of the narrow d band in Pt and Au, the density of states (DOS) at ϵ_F is high in Pt and low in Au. As a result a relatively small number of states (with the dominant sp symmetry) present at ϵ_F in Au contribute only weakly to α, despite large ξ_{Au}, while d states present at ϵ_F in Pt give a large contribution. For the same reason the SO coupling of the NM metal has a strong effect on the magnetic damping also for the Pd cap, while this effect is very weak for NM = Cu and Ag.

Although the SO coupling plays the dominant role in magnetic damping in Co/Pd and Co/Pt bilayers, the performed test calculations with $\xi_{NM} = 0$ show there is still a significant contribution to the enhancement of α due to the change of electronic structure in Co, invoked by the hybridization of quantum states at the Co/NM interface. This enhancement factor dominates for Co/NM bilayers with the cap of the NM metal (Cu, Ag, and Au) where the d band lies below ϵ_F; for such bilayers α shows a very similar dependence on the NM cap thickness (Fig. 10).

C. Layer contributions to the Gilbert damping

After having studied the film thickness dependence of the Gilbert damping constant in ferromagnetic films and Co/NM bilayers, a further investigation is needed to provide a deeper insight into the mechanism of magnetic damping in layered systems. In particular, it is worth understanding where the magnetic damping actually takes place and which part of the system plays a dominant role in the damping process. This problem has already been addressed to some extent above by investigating the effect of the SO coupling (its lack or presence) in the NM cap. Here, we analyze the Gilbert damping constant α by determining the contributions to α coming from individual atomic layers. These layer contributions are found as follows.

According to the general formula (9), the Gilbert damping constant α is proportional to the trace of the operator $D(\epsilon) = A^- L(\epsilon - H) A^+ L(\epsilon - H)$ at $\epsilon = \epsilon_F$ for $T = 0$ or to the integral $\int_{-\infty}^{\infty} \eta(\epsilon)\, \mathrm{tr} D(\epsilon)\, d\epsilon$ at finite temperature T. By introducing into $\mathrm{tr} D(\epsilon) = \sum_i \langle i|D(\epsilon)|i\rangle$ two unit operators $\sum_{n\boldsymbol{k}} |n\boldsymbol{k}\rangle\langle n\boldsymbol{k}| = 1$ built of the eigenstates $|n\boldsymbol{k}\rangle$ of the Hamiltonian, one finds, for any basis $|i\rangle$, that

$$\mathrm{tr} D(\epsilon) = \sum_i \sum_{n,n'} A^-_{i,n'\boldsymbol{k}} L[\epsilon - \epsilon_{n'}(\boldsymbol{k})] A^+_{n'\boldsymbol{k},n\boldsymbol{k}} \times L[\epsilon - \epsilon_n(\boldsymbol{k})] \langle n\boldsymbol{k}|i\rangle, \quad (17)$$

where $A^-_{i,n'\boldsymbol{k}} = \langle i|A^-|n'\boldsymbol{k}\rangle$ and $A^+_{n'\boldsymbol{k},n\boldsymbol{k}} = \langle n\boldsymbol{k}|A^-|n'\boldsymbol{k}\rangle^* = A_{nn'}(\boldsymbol{k})^*$. The expression (9) for the total damping constant α has been obtained with the basis $|i\rangle = |n\boldsymbol{k}\rangle$. However, taking the advantage of the trace invariance under the choice of basis, we can also calculate $\mathrm{tr} D(\epsilon)$ choosing the TB basis states $|i\rangle = |\boldsymbol{k} l \mu\sigma\rangle$ states, each of which is obtained by a combination of orbitals located on different atoms in the same layer l. In this way, we obtain

$$\mathrm{tr} D(\epsilon) = \sum_{\boldsymbol{k}\, l\mu\sigma} \sum_{n,n'} A^-_{\boldsymbol{k}l\mu\sigma,n'\boldsymbol{k}} A_{nn'}(\boldsymbol{k})^*\, a^{\sigma}_{nl\mu}(\boldsymbol{k})^* \times L[\epsilon - \epsilon_n(\boldsymbol{k})] L[\epsilon - \epsilon_{n'}(\boldsymbol{k})]. \quad (18)$$

Apart from the product of the two Lorentz functions and the matrix elements $A_{nn'}(\boldsymbol{k})$, the right-hand side of Eq. (18) also includes

$$A^-_{\boldsymbol{k}l\mu\sigma,n'\boldsymbol{k}} = \sum_{l'\mu'\sigma'} a^{\sigma'}_{n'l'\mu'}(\boldsymbol{k}) \langle \boldsymbol{k} l\mu\sigma|A^-|\boldsymbol{k}l'\mu'\sigma'\rangle = \xi_l \sum_{\mu'\sigma'} a^{\sigma'}_{n'l\mu'}(\boldsymbol{k}) \langle \mu\sigma|A^-_{\mathrm{at}}|\mu'\sigma'\rangle. \quad (19)$$

Substituting Eq. (19) into Eq. (18) one can write down the expression for the damping constant $\alpha \sim \int \eta(\epsilon) \mathrm{tr} D(\epsilon) d\epsilon$ as a sum of layer contributions α_l. Thus, we end up with the following breakdown of the Gilbert damping constant:

$$\alpha = \frac{1}{N_{\mathrm{FM}}} \sum_l \alpha_l, \quad (20)$$

where the layer contribution α_l is given explicitly as

$$\alpha_l = \frac{\pi \xi_l}{\mu_s} \frac{1}{\Omega_{\mathrm{BZ}}} \int d\boldsymbol{k} \sum_{n,n'} Q_{nn'l}(\boldsymbol{k})\, A_{nn'}(\boldsymbol{k})^*\, F_{nn'}(\boldsymbol{k}), \quad (21)$$

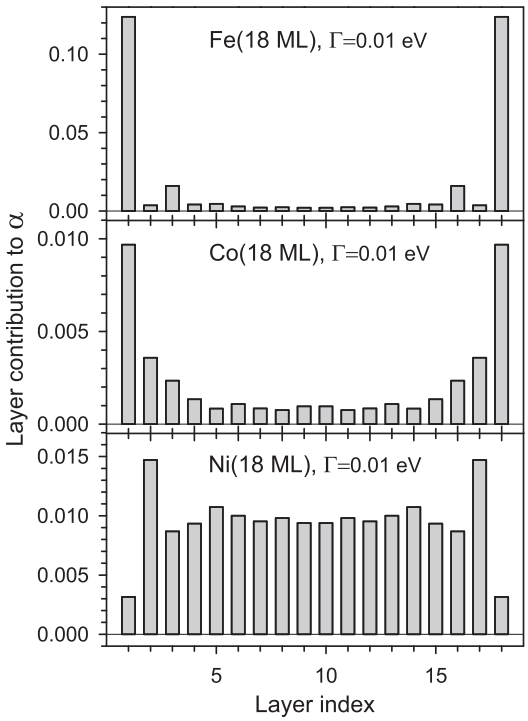

FIG. 12. Layer contributions to the Gilbert damping constant in Fe, Co, and Ni films of 18-ML thickness; $\Gamma = 0.01$ eV.

where

$$Q_{nn'l}(\boldsymbol{k}) = \sum_{\mu\sigma} \sum_{\mu'\sigma'} a^{\sigma}_{nl\mu}(\boldsymbol{k})^*\, a^{\sigma'}_{n'l\mu'}(\boldsymbol{k}) \langle \mu\sigma|A^-_{\mathrm{at}}|\mu'\sigma'\rangle. \quad (22)$$

Let us also note that $A_{nn'}(\boldsymbol{k})$, defined in Eq. (11), can also be calculated as

$$A_{nn'}(\boldsymbol{k}) = \sum_{l'} \xi_{l'} Q_{nn'l'}(\boldsymbol{k}). \quad (23)$$

In addition, this relation immediately proves that the sum (20) of the layer contributions (21) yields the total damping constant α given by Eq. (9).

The numerical calculation of α_l can also be speeded up by limiting the region of the integration over $\boldsymbol{k}$ in Eq. (21) to the 1/8 2D BZ instead of the whole BZ, which has been found not to alter the results for the investigated films and bilayers.

The layer contributions to the Gilbert damping in (001) bcc Fe, fcc Co, and fcc Ni films as well as in Co/NM bilayers with NM = Cu, Pt, and Au are shown in Figs. 12–14, respectively. For purely ferromagnetic Fe, Co, and Ni films the distribution of the layer contributions is symmetric with respect to the central symmetry plane of the film. For Fe and Co films the largest contributions come from the surface layers and for Co films they decline steadily to a minimum value when approaching the central layer(s). A similar increase of the layer contribution α_l is found at the (001) surface of the fcc Co semi-infinite crystal in Ref. [44] using a generalized formula for the Gilbert damping tensor and a different TB parametrization. In the case of Ni films the surface layers have the smallest contributions to the damping and the largest contributions come from the first subsurface layers ($l = 2$ and $N - 1$). As seen in Figs. 13 and 14, adding a NM cap to the Co

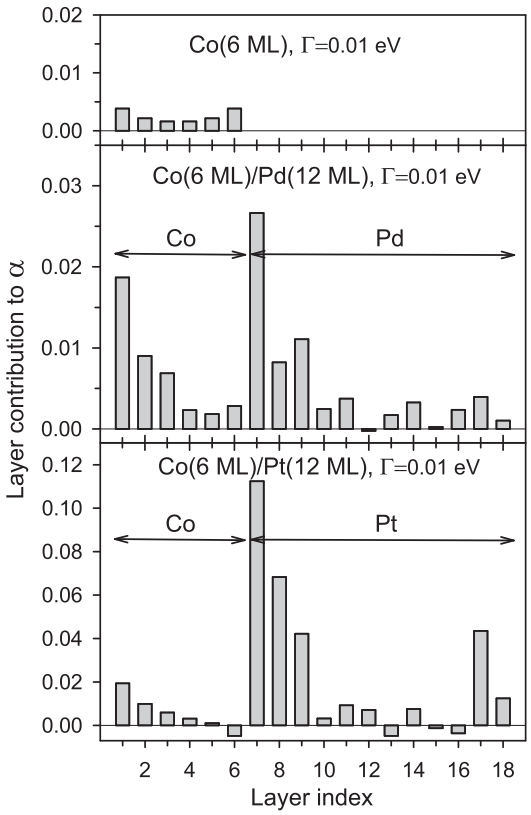

FIG. 13. Layer contributions to the Gilbert damping constant in Co(6 ML) film as well as in Co(6 ML)/Pd(12 ML), and Co(6 ML)/Pt(12 ML) bilayers; $\Gamma = 0.01$ eV.

film not only alters the symmetric distribution of the damping in the pure Co film but it also increases the overall contribution stemming from the Co part of the film. This is caused by change of the electronic structure in Co due to adding the NM cap. The asymmetric distribution of damping layer contributions in the Co film is very similar in all investigated Co/NM bilayers (with the exception of the interface Co layer) and it is very weakly affected by the thickness of the NM cap. Let us also note that small negative contributions α_l are obtained for some l in the bilayer systems since the applied method of the layer-resolved breakdown of the damping constant does not guarantee the positive sign of all α_l though the total α_l is positive according to Eq. (9).

The layer contributions α_l inside the NM caps of metals with the top of the d band below ϵ_F are much smaller than in the Pd or Pt caps. They are marginal in the Cu and Ag caps so that the Gilbert damping in the Co/Cu and Co/Ag bilayers comes almost entirely from the Co film. In the case of the Au cap the very interface Au atomic layer contributes to the damping significantly, as strongly as the surface Co layer; see Fig 14. This is a result of large SO coupling of Au and, presumably, an increase of the local DOS in the Au interface layer due to the hybridization of s, p states in Au with d states in Co across the Co/Au interface. For Co/NM bilayers with nonmagnetic metals like Pd and Pt, whose d band crosses ϵ_F, the dominant contributions to the damping come from the NM caps. In such bilayers the majority of damping originates from a few atomic layers of the NM cap that are closest to the Co/NM interface. Surprisingly, significant contributions also come from few most external layers of the NM cap.

The damping contribution in the Pd and Pt caps is largest at the Co/NM interface (NM = Pd or Pt) atomic layer $l = l_1^{\mathrm{NM}}$ and it decays with the increasing distance $z = z_l = (l - l_1^{\mathrm{NM}})a/2$ from the interface (Fig. 15). The obtained

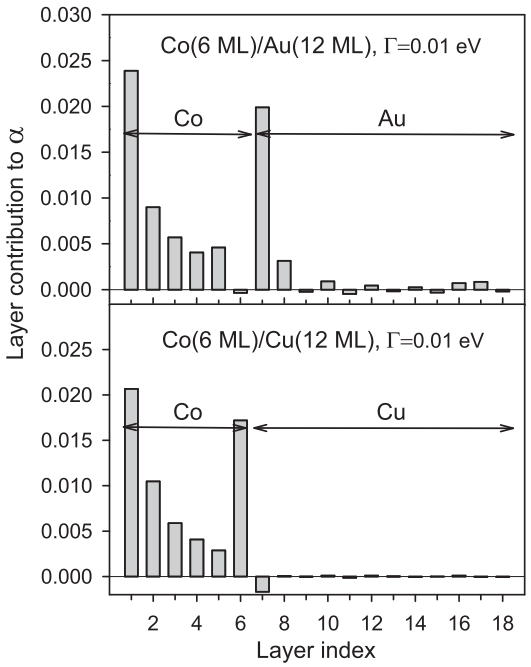

FIG. 14. Layer contributions to the Gilbert damping constant in Co(6 ML)/NM(12 ML) bilayers (NM = Cu, Au); $\Gamma = 0.01$ eV.

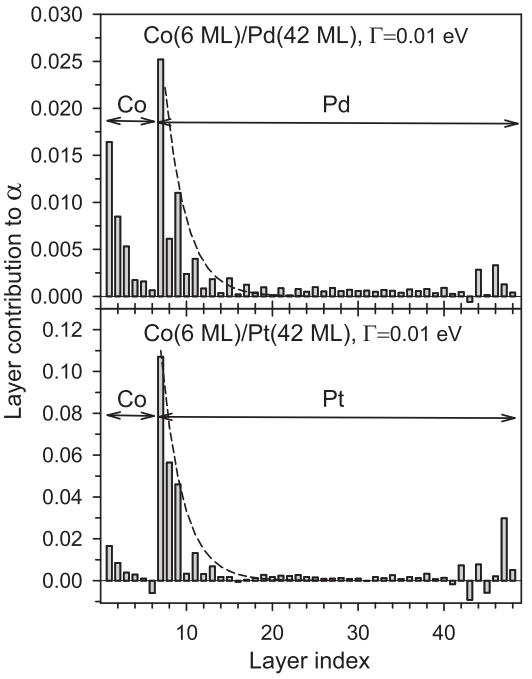

FIG. 15. Layer contributions to the Gilbert damping constant in Co(6 ML)/NM(42 ML) bilayers (NM = Pd, Pt); $\Gamma = 0.01$ eV. The dashed line marks a fit with the function $\alpha_7 \exp(-z_l/\lambda)$ with $\lambda = 0.45$ nm inside the NM (see text).

decay of $\alpha_l \equiv \rho_\alpha(z = z_l)$, though not strictly monotonic, can be roughly approximated with an exponential function $\rho_\alpha = \rho_\alpha(z = 0)e^{-z/\lambda}$. This can be argued to be related to similar dependence obtained in the spin-pumping theory for the magnetization density $\mu(z)$ induced in the NM cap by the precessing magnetization in the ferromagnet in the presence of a spin-flip mechanism in the NM. In the spin-pumping approach, the exponential decay of $\mu(z) \sim e^{-z/\lambda_{sd}}$ holds if the spin-diffusion length λ_{sd} in the NM is much smaller than the NM cap thickness $L = N_{NM}a/2$. While the direct identification of λ with λ_{sd} is not certain at present, the obtained approximate value of $\lambda = 0.45$ nm for both Pd and Pt is in good agreement with the recently measured value of $\lambda_{sd}^{Pt} = 0.5 \pm 0.3$ nm [28] for Pt but it is significantly smaller than the values $\lambda_{sd}^{Pd} = 2.0 \pm 0.09$ nm [74] and $\lambda_{sd}^{Pd} = 2.6 \pm 0.12$ nm [28] found experimentally for Pd.

IV. CONCLUSIONS

The Gilbert damping constant is presently calculated for bulk ferromagnetic metals, their films, and Co/NM bilayers using the torque-correlation model within the TB formalism. The calculations are performed for systems up to 48 ML thick thanks to employing finite temperature which leads to a faster convergence of the numerical integration over the BZ as well as replacing of the involved energy integral by the equivalent sum over Matsubara frequencies. The calculated damping constant depends, often in a nonmonotonic way, on the thickness of FM films and it tends to the bulk value α_b for large thicknesses. However, the rate of convergence to α_b varies largely with metal and depends strongly on the scattering rate Γ. In some cases it is so slow that α does not saturate at α_b within the investigated range of thicknesses and the saturation thickness is expected to be a few hundred ML. The dependence of the damping constant α on the thicknesses N_{FM} and N_{NM} of FM films and NM caps, respectively, has characteristic oscillations due to QW states and their amplitude becomes negligible at N_{FM} and N_{NM} larger than 20 ML.

The obtained results show that the Gilbert damping constant α can be largely modified in pure FM films, in comparison with the corresponding bulk metals, so that α is reduced or enhanced depending on the value of Γ. In the investigated Co/NM bilayer systems, the calculated damping constant α shows a significant enhancement in comparison with pure Co films and bulk fcc Co and it is particularly strong for Pd and Pt caps. This effect is found for the NM caps as thin as 1 ML and the damping constant apparently saturates at a final value after adding just a few ML if small QW oscillations are disregarded. However, due to the limited range of investigated NM thicknesses (up to 22 ML) we expect that the convergence of α does not actually take places within this range for Cu, Ag, and Au since the spin-diffusion lengths of these *sp* metals are of the order of 100 nm.

The obtained linear dependence of the Gilbert damping against the inverse of Co thickness for Co/NM bilayers agrees well with experiment. It should be noted that in the present model the inverse proportionality of the damping enhancement with the FM film thickness is a result of our numerical calculations. This result confirms the approach of spin pumping theory where such thickness dependence is built in as an underlying assumption. It is also clearly demonstrated, by switching off and on the SO coupling in the NM, that the enhancement of the damping in the Co/Pd and Co/Pt bilayers comes mainly from the NM cap while in the Co/Cu and Co/Ag bilayers with the *sp* metal cap the obtained enhancement results merely from modification of the electronic structure in the Co film. The nonlocal origin of the additional damping in the Co/Pd and Co/Pt bilayers is confirmed by distribution of layer contributions to the damping constant which are largest in a few atomic layers of the Pd and Pt caps close to the Co/NM interface. Such layer contributions are found to be very small in the Cu and Ag caps. The Au cap is a borderline case as a significant contribution comes from the Au atomic layer at the very Co/Au interface.

The present calculations show that the strong enhancement of magnetic damping in Co/Pd and Co/Pt bilayers results from the combination of two properties of the NM: the large SO coupling and the large DOS at the Fermi level ϵ_F. This conclusion can be compared with the spin pumping theory [36] where the magnetic damping in FM/NM systems depends on several phenomenological parameters, describing the diffusion of conduction electrons, the efficiency of the spin-flip process, as well as the mixing conductance $g_r^{\uparrow\downarrow}$ of the FM/NM interface. While the diffusion coefficient is related to the electron-scattering rate Γ and the spin-flip relaxation time τ_{sf} depends on the strength of the SO coupling in the NM, there is no immediate relation between the mixing conductance $g_r^{\uparrow\downarrow}$ and the DOS in the NM. Such relation is not likely to exist since $g_r^{\uparrow\downarrow}$ depends on how states in the FM match states in the NM across the FM/NM interface which is not directly related to the number of states available for conducting electrons at ϵ_F in the NM. The lack of such relation is confirmed by the results reported in Ref. [38].

In summary, the obtained results for the Gilbert damping constant and its analysis, in particular the breakdown in the real space into layer contributions, lead to better understanding mechanisms of the magnetic damping in FM films and FM/NM layered systems.

ACKNOWLEDGMENTS

Two of us (E.B. and M.C.) acknowledge the financial support of the Foundation for Polish Science within the International PhD Projects Programme, cofinanced by the European Regional Development Fund within Innovative Economy Operational Programme "Grants for Innovation."

APPENDIX: MATSUBARA FREQUENCY METHOD

As has previously been mentioned, the efficiency of our calculations is significantly improved by introducing finite temperature into the electronic occupation factors and subsequent summation over the Matsubara frequencies.

This is achieved by using an analytical expression for the integral defining the factor $F_{nn'}(\boldsymbol{k})$ in Eq. (14). This expression is derived by replacing the integral over the energy with the integral over a finite closed contour in the upper complex half plane (including the real axis) and by making use of the

residue theorem. The contour integral can be expressed as the sum

$$F_{nn'}(\boldsymbol{k}) = \oint F(z)\,dz = 2\pi i \sum_{j=1}^{N} a_{-1}^{j}$$
$$= 2\pi i\left(a_{-1}(z_1) + a_{-1}(z_1') + \sum_{k=0}^{\infty} a_{-1}(\omega_k)\right) \quad \text{(A1)}$$

of the residues of the integrand $F(z) = \eta(z)L(z-\epsilon_n)L(z-\epsilon_{n'})$ at its poles lying in the upper half plane. The poles of the Lorentz functions, $L(z-\epsilon_n)$ and $L(z-\epsilon_{n'})$, are

$$z_1 = \epsilon_n + i\Gamma/2, \quad \text{(A2a)}$$
$$z_2 = \epsilon_n - i\Gamma/2 \quad \text{(A2b)}$$

and

$$z_1' = \epsilon_{n'} + i\Gamma/2, \quad \text{(A3a)}$$
$$z_2' = \epsilon_{n'} - i\Gamma/2, \quad \text{(A3b)}$$

respectively. The Fermi-Dirac distribution function,

$$f_{\mathrm{FD}}(z) = \frac{1}{1+e^{\beta(z-\epsilon_{\mathrm{F}})}}, \quad \text{(A4)}$$

with $\beta = 1/k_{\mathrm{B}}T$, has poles at complex energies

$$\omega_k = \epsilon_{\mathrm{F}} + i\pi(2k+1)k_{\mathrm{B}}T \quad \text{(A5)}$$

($k = 0, \pm 1, \pm 2, \ldots$) which are called the Matsubara frequencies. Around the poles, the function $f_{\mathrm{FD}}(z)$ and its negative derivative $\eta(z) = -df_{\mathrm{FD}}(z)/dz$ behave as

$$f_{\mathrm{FD}}(z) = \frac{1}{\beta}\frac{1}{z-\omega_k}, \quad \text{(A6)}$$

$$\eta(z) = \frac{1}{\beta}\frac{1}{(z-\omega_k)^2}. \quad \text{(A7)}$$

Thus, the Matsubara frequencies are the first-order poles of $f_{\mathrm{FD}}(z)$ and the second-order poles of its derivative $\eta(z)$.

The residues of the function $F(z)$ at the poles z_1, z_1', and ω_k (which lie in the upper complex half plane) are

$$a_{-1}(z_1) = \frac{\Gamma}{2\pi}\frac{\eta(z_1)L(z_1-\epsilon_{n'})}{z_1-z_2}, \quad \text{(A8a)}$$
$$a_{-1}(z_1') = \frac{\Gamma}{2\pi}\frac{\eta(z_1')L(z_1'-\epsilon_{n})}{z_1'-z_2'}, \quad \text{(A8b)}$$

and

$$a_{-1}(\omega_k) = \frac{\Gamma^2}{2\beta\pi^2 C_k}\left(\frac{C_{2k}+C_{2k}'}{C_{2k}C_{2k}'} + \frac{i\Gamma}{2C_k}(C_{1k}C_{2k}+C_{1k}'C_{2k}')\right) \quad \text{(A9)}$$

with $C_{ik} = \omega_k - z_i$, $C_{ik}' = \omega_k - z_i'$, and $C_k = C_{1k}C_{2k}C_{1k}'C_{2k}'$. Having calculated the residues we can now evaluate the integral in Eq. (A1). Then, substituting the expressions (A8a), (A8b), and (A9) obtained for the residues we arrive at the sought analytical expression for the factor,

$$F_{nn'}(\boldsymbol{k}) = J_1 + iJ_2, \quad \text{(A10)}$$

where

$$J_1 = \frac{\Gamma}{2\pi}\frac{\eta(z_1)+\eta(z_1')}{(\epsilon_n-\epsilon_{n'})^2+\Gamma^2} - \frac{\Gamma^3}{2\pi\beta}\sum_{k=0}^{\infty}\frac{C_{1k}C_{2k}+C_{1k}'C_{2k}'}{C_k^2}, \quad \text{(A11a)}$$

$$J_2 = -\frac{\Gamma^2}{2\pi}\frac{1}{(\epsilon_n-\epsilon_{n'})^2+\Gamma^2}\frac{\eta(z_1')-\eta(z_1)}{z_1'-z_1} + \frac{\Gamma^2}{\pi\beta}\sum_{k=0}^{\infty}\frac{C_{2k}+C_{2k}'}{C_kC_{2k}C_{2k}'}. \quad \text{(A11b)}$$

Note that both J_1 and J_2 are complex numbers.

The difference quotient in Eq. (A11b) becomes ill defined numerically if the energies $\epsilon_n, \epsilon_{n'}$ are very close to each other or equal, in particular, for $n = n'$. To avoid numerical problems the function $\eta(z')$ is expressed as the Taylor series around $z = z_1$. Thus, we obtain the following expression:

$$R = \frac{\eta(z_1')-\eta(z_1)}{z_1'-z_1} = \frac{d\eta(z)}{dz}|_{z=z_1} + \sum_{m=2}^{\infty}\frac{1}{m!}\frac{d^m\eta(z)}{dz^m}|_{z=z_1}(z_1'-z_1)^{m-1}, \quad \text{(A12)}$$

which converges quickly if $\beta|\epsilon_{n'}-\epsilon_n| \ll 1$. It is found that terms up to $m = 6$ are sufficient, if $\beta|\epsilon_{n'}-\epsilon_n| < 0.01$, to get full convergence of R in our numerical calculations. The derivatives $\eta^{(m)}(z) = d^m\eta(z)/dz^m$ can be found from the following relation:

$$\eta = \beta f(1-f) \quad \text{(A13)}$$

where $f = f_{\mathrm{FD}}$. Its application leads to a recursive expression for $\eta^{(m)}$ in terms of $f, \eta, \ldots, \eta^{(m-1)}$ as follows:

$$\eta^{(m)} = -\beta\sum_{k=0}^{m}\binom{m}{k}f^{(k)}f^{(m-k)} + \beta f^{(m)} = -\beta\sum_{k=1}^{m-1}\binom{m}{k}\eta^{(k-1)}\eta^{(m-k-1)} - \beta(1-2f)\eta^{(m-1)}, \quad \text{(A14)}$$

where $f^{(k)}$ has been replaced with $-\eta^{(k-1)}$ for $k \geqslant 1$. In particular we find

$$\eta' = -\beta(1-2f)\eta\,, \quad \text{(A15a)}$$
$$\eta'' = -2\beta\eta\eta - \beta(1-2f)\eta', \quad \text{(A15b)}$$
$$\eta''' = -6\beta\eta\eta' - \beta(1-2f)\eta''. \quad \text{(A15c)}$$

In this way, we can evaluate the integral in Eq. (14) analytically by employing the Matsubara frequency method and perform the numerical calculation of the Gilbert damping constant at finite temperature in an effective way. We have found that, for the applied temperature $T = 300$ K, the infinite series in Eqs. (A11a) and (A11b) can be truncated to the sum of the first 40 terms ($k = 1,2,\ldots,40$) without losing numerical accuracy.

[1] S. Mangin, D. Ravelosona, J. A. Katine, M. J. Carey, B. D. Terris, and E. E. Fullerton, Nat. Mater. **5**, 210 (2006).
[2] T. L. Gilbert, Phys. Rev. **100**, 1243 (1955).
[3] T. L. Gilbert, IEEE Trans. Magn. **40**, 3443 (2004).
[4] S. S. P. Parkin, M. Hayashi, and L. Thomas, Science **320**, 190 (2008).
[5] V. Kamberský, Czech. J. Phys. B **26**, 1366 (1976).
[6] V. Kamberský, Phys. Rev. B **76**, 134416 (2007).
[7] N. Nakabayashi, A. Takeuchi, K. Hosono, K. Taguchi, and G. Tatara, Phys. Rev. B **82**, 014403 (2010).
[8] A. T. Costa, R. B. Muniz, S. Lounis, A. B. Klautau, and D. L. Mills, Phys. Rev. B **82**, 014428 (2010).
[9] D. L. R. Santos, P. Venezuela, R. B. Muniz, and A. T. Costa, Phys. Rev. B **88**, 054423 (2013).
[10] R. Arias and D. L. Mills, Phys. Rev. B **60**, 7395 (1999).
[11] P. Landeros, R. E. Arias, and D. L. Mills, Phys. Rev. B **77**, 214405 (2008).
[12] Kh. Zakeri, J. Lindner, I. Barsukov, R. Meckenstock, M. Farle, U. von Hörsten, H. Wende, W. Keune, J. Rocker, S. S. Kalarickal, K. Lenz, W. Kuch, K. Baberschke, and Z. Frait, Phys. Rev. B **76**, 104416 (2007).
[13] Th. Gerrits, M. L. Schneider, and T. J. Silva, J. Appl. Phys. **99**, 023901 (2006).
[14] W. Platow, A. N. Anisimov, G. L. Dunifer, M. Farle, and K. Baberschke, Phys. Rev. B **58**, 5611 (1998).
[15] Z. Celinski and B. Heinrich, J. Appl. Phys. **70**, 5935 (1991).
[16] B. Heinrich, K. B. Urquhart, A. S. Arrott, J. F. Cochran, K. Myrtle, and S. T. Purcell, Phys. Rev. Lett. **59**, 1756 (1987).
[17] A. Barman, S. Wang, O. Hellwig, A. Berger, E. E. Fullerton, and H. Schmidt, J. Appl. Phys. **101**, 09D102 (2007).
[18] P. He, X. Ma, J. W. Zhang, H. B. Zhao, G. Lüpke, Z. Shi, and S. M. Zhou, Phys. Rev. Lett. **110**, 077203 (2013).
[19] R. Urban, G. Woltersdorf, and B. Heinrich, Phys. Rev. Lett. **87**, 217204 (2001).
[20] S. Mizukami, Y. Ando, and T. Miyazaki, J. Magn. Magn. Mater. **226-230**, 1640 (2001); Jpn. J. Appl. Phys., Part 1 **40**, 580 (2001).
[21] S. Mizukami, Y. Ando, and T. Miyazaki, Phys. Rev. B **66**, 104413 (2002).
[22] S. Mizukami, E. P. Sajitha, D. Watanabe, F. Wu, T. Miyazaki, H. Naganuma, M. Oogane, and Y. Ando, Appl. Phys. Lett. **96**, 152502 (2010).
[23] S. Mizukami, X. Zhang, T. Kubota, H. Naganuma, M. Oogane, Y. Ando, and T. Miyazaki, Appl. Phys. Express **4**, 013005 (2011).
[24] P. Lubitz, S. F. Cheng, and F. J. Rachford, J. Appl. Phys. **93**, 8283 (2003).
[25] J. Walowski, M. Djordjevic, B. Lenk, C. Hamann, J. McCord, and M. Münzenberg, J. Phys. D: Appl. Phys. **41**, 164016 (2008).
[26] X. Liu, W. Zhang, M. J. Carter, and G. Xiao, J. Appl. Phys. **110**, 033910 (2011).
[27] M. Charilaou, K. Lenz, and W. Kuch, J. Magn. Magn. Mater. **322**, 2065 (2010).
[28] C. T. Boone, H. T. Nembach, J. M. Shaw, and T. J. Silva, J. Appl. Phys. **113**, 153906 (2013).
[29] G. H. O. Daalderop, P. J. Kelly, and F. J. A. den Broeder, Phys. Rev. Lett. **68**, 682 (1992).
[30] P. F. Carcia, J. Appl. Phys. **63**, 5066 (1988).
[31] D. Weller, Y. Wu, J. Stohr, M. G. Samant, B. D. Hermsmeier, and C. Chappert, Phys. Rev. B **49**, 12888 (1994).
[32] S. Uba, L. Uba, A. N. Yaresko, A. Ya. Perlov, V. N. Antonov, and R. Gontarz, Phys. Rev. B **53**, 6526 (1996).
[33] L. Berger, Phys. Rev. B **54**, 9353 (1996).
[34] E. Šimánek and B. Heinrich, Phys. Rev. B **67**, 144418 (2003).
[35] D. L. Mills, Phys. Rev. B **68**, 014419 (2003).
[36] Y. Tserkovnyak, A. Brataas, and G. E. W. Bauer, Phys. Rev. Lett. **88**, 117601 (2002); Phys. Rev. B **66**, 224403 (2002); J. Appl. Phys. **93**, 7534 (2003).
[37] T. Yoshino, K. Ando, K. Harii, H. Nakayama, Y. Kajiwara, and E. Saitoh, Appl. Phys. Lett. **98**, 132503 (2011).
[38] M. Zwierzycki, Y. Tserkovnyak, P. J. Kelly, A. Brataas, and G. E. W. Bauer, Phys. Rev. B **71**, 064420 (2005).
[39] K. Gilmore, Y. U. Idzerda, and M. D. Stiles, Phys. Rev. Lett **99**, 027204 (2007).
[40] I. Garate and A. MacDonald, Phys. Rev. B **79**, 064403 (2009); **79**, 064404 (2009).
[41] I. Garate, K. Gilmore, M. D. Stiles, and A. H. MacDonald, Phys. Rev. B **79**, 104416 (2009).
[42] H. Ebert, S. Mankovsky, D. Ködderitzsch, and P. J. Kelly, Phys. Rev. Lett. **107**, 066603 (2011).
[43] E. Barati, M. Cinal, D. M. Edwards, and A. Umerski, EPJ Web Conf. **40**, 18003 (2013).
[44] D. Thonig and J. Henk, New J. Phys. **16**, 013032 (2014).
[45] S. Mankovsky, D. Ködderitzsch, G. Woltersdorf, and H. Ebert, Phys. Rev. B **87**, 014430 (2013).
[46] C. Liu, C. K. A. Mewes, M. Chshiev, T. Mewes, and W. H. Butler, Appl. Phys. Lett. **95**, 022509 (2009).
[47] I. Barsukov, S. Mankovsky, A. Rubacheva, R. Meckenstock, D. Spoddig, J. Lindner, N. Melnichak, B. Krumme, S. I. Makarov, H. Wende, H. Ebert, and M. Farle, Phys. Rev. B **84**, 180405(R) (2011).
[48] D. M. Edwards and O. Wessely, J. Phys.: Condens. Matter **21**, 146002 (2009).
[49] Z. Li and S. Zhang, Phys. Rev. Lett. **92**, 207203 (2004).
[50] S. Zhang and Z. Li, Phys. Rev. Lett. **93**, 127204 (2004).
[51] E. Barati, M. Cinal, D. M. Edwards, and A. Umerski, in *Ultrafast Magnetism I - Proceedings of Ultrafast Magnetism Conference (UMC 2013), Strasbourg, France, October 28–November 1, 2013*, Springer Proceedings in Physics, Vol. 159, edited by J.-Y. Bigot, W. Hübner, T. Rasing, and R. Chantrell (Springer International Publishing, Cham, 2015).
[52] J. C. Slater and G. F. Koster, Phys. Rev. **94**, 1498 (1954).
[53] D. A. Papaconstantopoulos, *Handbook of the Band Structure of Elemental Solids* (Plenum, New York, 1986).
[54] H. Shiba, Progr. Theor. Phys. **46**, 77 (1971).
[55] H. L. Skriver, *The LMTO Method* (Springer-Verlag, Berlin, 1984).
[56] M. Cinal, D. M. Edwards, and J. Mathon, Phys. Rev. B **50**, 3754 (1994).
[57] J. Mathon, Murielle Villeret, A. Umerski, R. B. Muniz, J. d'Albuquerque e Castro, and D. M. Edwards, Phys. Rev. B **56**, 11797 (1997).
[58] M. Cinal, J. Phys.: Condens. Matter **15**, 29 (2003).
[59] M. Cinal and D. M. Edwards, Phys. Rev. B **55**, 3636 (1997).
[60] A. R. Mackintosh and O. K. Andersen, *Electrons at Fermi Surface* (Cambridge University Press, Cambridge, England, 1980).
[61] E. Abate and M. Asdente, Phys. Rev. **140**, A1303 (1965).

[62] Ch. Li, A. J. Freeman, H. J. F. Jansen, and C. L. Fu, Phys. Rev. B **42**, 5433 (1990).
[63] K. Gilmore, Y. U. Idzerda, and M. D. Stiles, J. Appl. Phys. **103**, 07D303 (2008).
[64] S. S. P. Parkin, N. More, and K. P. Roche, Phys. Rev. Lett. **64**, 2304 (1990).
[65] D. M. Edwards, J. Mathon, R. B. Muniz, and M. S. Phan, Phys. Rev. Lett. **67**, 1476 (1991).
[66] L. Szunyogh, B. Újfalussy, C. Blaas, U. Pustogowa, C. Sommers, and P. Weinberger, Phys. Rev. B **56**, 14036 (1997).
[67] M. Cinal and D. M. Edwards, Phys. Rev. B **57**, 100 (1998).
[68] M. Cinal, J. Phys.: Condens. Matter **13**, 901 (2001).
[69] M. Cinal and A. Umerski, Phys. Rev. B **73**, 184423 (2006).
[70] J. Li, M. Przybylski, F. Yildiz, X. D. Ma, and Y. Z. Wu, Phys. Rev. Lett. **102**, 207206 (2009).
[71] U. Bauer, M. Dąbrowski, M. Przybylski, and J. Kirschner, Phys. Rev. B **84**, 144433 (2011).
[72] M. Przybylski, M. Dąbrowski, U. Bauer, M. Cinal, and J. Kirschner, J. Appl. Phys. **111**, 07C102 (2012).
[73] A. M. N. Niklasson, S. Mirbt, H. L. Skriver, and B. Johansson, Phys. Rev. B **56**, 3276 (1997).
[74] K. Kondou, H. Sukegawa, S. Mitani, K. Tsukagoshi, and S. Kasai, Appl. Phys. Express **5**, 073002 (2012).